Noble gas in oil and gas accumulations

Alain Prinzhofer

The specific properties of noble gas isotopes (chemical inertness, high potential for source characterization, simple physical properties) have been recognized to be of great interest for natural gas characterization. The pioneering work of the Californian Institute of Technology (Zartman and Wasserburg, 1961; Wasserburg *et al.*, 1963) presented most of the basic concepts which have been developed in the following 50 years of noble gas geochemistry for hydrocarbon accumulations (non-organic origins of noble gases, chronology of accumulation, crustal versus mantle contamination, meteoric water influence, in situ versus ex situ noble gas exchange with fluids, etc…). Few papers were published in the decades following this application of noble gases (Nagao et al., 1981; Sano et al., 1982; Oxburg et al., 1986; Mazor and Bosh, 1987; Bosh and Mazor, 1988; Jenden et al., 1988). Only recently, in the past 20 years or so, have a large number of publications from different academic centers shown renewed interest in this methodology with an exponential increase in applications (Ballentine et al., 1991; O'Nions and Ballentine, 1993; Ballentine and O'Nions, 1994; Sherwood-Lollar et al., 1994; Xu et al., 1995; Ballentine et al., 1996; Torgersen and Kennedy, 1999; Battani et al., 2000; Kennedy et al., 2002; Ballentine and Sherwood Lollar, 2002; Prinzhofer and Battani, 2003; Kotarba and Nagao, 2008; Yu et al., 2010). The last decade confirms this trend, with several scientific groups proposing noble gas geochemical services for commercial oil and gas companies. Very recent interest in shale gas exploration confirms and increases this tendency for further commercial applications of noble gas geochemistry in the petroleum and natural gas industry.

A-Introduction : the possible sources and physical processes that may affect HC-associated noble gas isotopes

A.1- The three main sources of noble gas isotopes in petroleum and gas systems

Noble gas compounds represent a simple family of chemical elements and isotopes, with only five elements (He, Ne, Ar, Kr, Xe with the exception of radon, which has such a short half life that its study represents a distinct and different interest for geologists) and a large number of isotopes, for which only four isotopic ratios are generally used for oil and gas exploration: $^{3}He/^{4}He$, $^{20}Ne/^{22}Ne$, $^{21}Ne/^{22}Ne$ and $^{40}Ar/^{36}Ar$. Considering only subsurface fluids (oil, gas, water), only three main terrestrial reservoirs are implied in noble gas generation (Figure 1):

- *Air Saturated Water (ASW)*
  The ASW reservoir (Air Saturated Water) corresponds to the noble gases present in the subsurface waters, which were previously equilibrated with the atmosphere, via recharge zones of aquifers. Knowing the composition of the atmosphere in terms of concentrations and isotopic ratios of noble gases, and the solubility coefficients between gas and water, it is possible to calculate the composition of this ASW reservoir. The only unknown parameter is the equilibration temperature at the time of

the recharge. However, although this variation is paramount when calculating paleo-temperatures (Weis, 1970, 1971; Weis and Kyser, 1978; Kipfer et al., 2002), the variation in concentrations is generally sufficiently small to be neglected in petroleum geochemistry, as other processes of exchange between water and hydrocarbons present much larger fractionations than this second order variation.

- *Radiogenic isotopes*

  The radiogenic or nucleogenic contribution comes from minerals. Several nuclear reactions, including the natural radioactive decay of some isotopes in minerals, as well as some nucleogenic reactions may generate excesses of certain noble gas isotopes. The two most important are the production of ^{4}He, due mainly to the radioactive decay of uranium and thorium (and any other α production radioactive process), and ^{40}Ar, generated as the residue of the natural radioactive decay of ^{40}K (another part generating ^{40}Ca). Other isotopes may be generated by more complex processes involving the interaction between neutrons and isotopes of various chemical compounds. The main noble gas isotopes generated through nucleogenic processes are ^{3}He, ^{21}Ne and ^{22}Ne (Morrison and Pine, 1955; Sarda et al., 1988; Kennedy et al., 1990; Moreira and Allegre, 1998; Ballentine and Burnard, 2002). All these noble gas isotopes generated through geological time originate in minerals, which may be present in the sedimentary series, or from deeper horizons such as the metamorphic part of the crust, and the crustal basement composed of various igneous and metamorphic rocks of different ages. Compare to sedimentary minerals, the continental basement is generally older, and with higher concentrations of the radioactive elements U, Th, K, resulting in greater concentrations of radiogenic isotopes, concentrated mainly in the upper 10km of the continental crust. Rudnick and Fountain (1995) calculate that 66% of the radiogenic/nucleogenic budget is concentrated in the 10-15km top kilometers of the crust, 28% at intermediate depths of 10-15km to 20-25km, and that only 6% of the radiogenic production is generated in the lower part of the crust, i.e. below 25km. The mechanisms - and their efficiencies - that allow these isotopes to migrate from the basement up to an oil or gas accumulation located in sedimentary series are the limiting processes for the abundance of these isotopes in petroleum systems.

- *Mantle fluids*

  It was discovered some decades ago that in some sedimentary basins, a clear presence of mantle fluids may be demonstrated (Oxburg et al., 1986; O'Nions and Oxburg, 1988). The mantle fluids have a significantly different signature from the other reservoirs in terms mainly of noble gas isotopic ratios. The most commonly used is the $^{3}He/^{4}He$ ratio, which is highly enriched in ^{3}He in the mantle. Normalized to the air value of $1.4\ 10^{-6}$, the upper mantle has values between 6 and 8 times the atmospheric value depending on its location in the mantle: $8Ra \pm 2$ is the accepted value for MORB (Kurz and Jenkins, 1981; Graham, 2002), whereas a sub-continental upper mantle has a lower value around 6Ra (Dunai and Baur, 1995). The ASW isotopic ratio is of course the air ratio of $1.4\ 10^{-6}$, as there is no measurable isotopic fractionation for helium between a water and vapor phase. However, due to the very low concentration of helium in the air (5ppm) and its lower solubility coefficient in water compared with other noble gases, the contribution of ASW helium is generally neglected in geologic petroleum reservoirs. Only in superficial gas seeps may this contribution be significant compared to other sources. The $^{3}He/^{4}He$ signature of crustal sources, either

sedimentary or from the basement, is around 0.02Ra. The lower mantle, possibly visible through hot spots, has helium isotopic ratios as high as 50 Ra (Stuart et al., 2003). The neon isotopes have also been extensively studied in mantle sources (Sarda et al., 1988; Honda et al., 1991; Moreira and Allegre, 1998; Trieloff et al., 2000, 2002; Ballentine et al., 2005). The values for the ratios $^{20}Ne/^{22}Ne$ and $^{21}Ne/^{22}Ne$ vary between 12.5 to 13.8 and 0.06 to 0.063 respectively. The $^{40}Ar/^{36}Ar$ isotopic ratios are also very different in the mantle reservoir, as ^{36}Ar is extremely depleted in the mantle. The measured ratios may be as high as 30,000 (Staudacher et al., 1989) or even 40,000 (Burnard et al., 1997).

A summary of the noble gas signatures of these different reservoirs is presented in Table 1, and a schematic sketch of their contribution in an hydrocarbon accumulation is represented in Figure 1 (from Ballentine and O'Nions, 1994, modified).

A.2- The three main processes affecting noble gas isotopes

Because all the noble gas compounds are strictly chemically inert under geological conditions, only physical processes may affect and fractionate their proportions. I presented in the previous paragraph the nuclear processes generating the radiogenic and nucleogenic noble gas isotopes, and I will deal in this chapter only with non-nuclear physical processes. It is possible to distinguish only three kinds:

Exchange of noble gas compounds between phases

The noble gas compounds may originally be present in a gas phase (atmosphere, natural gas accumulations) a liquid phase (water, oil) or a solid phase (minerals with radioactive elements, surface adsorption, hydrates). The hydrocarbon fluids, oil or gas, come principally from degradation of fossil organic matter, and are generated almost without any noble gas content, as the organic matter does not contain gas compounds, and generally almost no radioactive compounds (Ricard et al., 2011). However, the associated shales, rich in organic matter, have generally high concentrations in Uranium and Thorium, resulting in a potential radiogenic contribution to the hydrocarbon fluids from the source rocks (Torgersen and Kennedy, 1999). If noble gases are enriched in an oil or gas phase in the subsurface, this largely results from their exchange between phases, quantified by partition coefficients called either solubility coefficients or Henry coefficients. The phases encountered by hydrocarbons may be either water, or supercritical mantle and hydrothermal fluids, mainly composed of H_2O and CO_2. Another possible exchange between phases, not yet documented in Earth Sciences, is the exchange between fluid phases and hydrates. It is important to note that in the case of hydrate formation, the stability of heavy noble gas hydrates is much larger than the better known stabilities of CH_4 and CO_2 hydrates (Berecz and Balla-Achs, 1983; Dyadin et al., 1996). The occurrence of hydrates, either on the sea floor or in peri-glacial areas, have the potential for drastically fractionating the heavy nobles gases (trapped in the hydrate solid phase) versus the light noble gases (never stable in hydrates at natural conditions). However, no quantitative study of these fractionations has been carried so far in Earth Sciences.

The solubility coefficients of noble gases between a gas phase and a water phase have been extensively studied versus temperature and pressure (Crovetto et al., 1981. Smith and Kennedy, 1983. Smith, 1985. Harvey, 1998), and a summary of the values are presented in Table 2. The solubilities may be expressed as Henry's pressures or solubility coefficients. The

Henry pressure (expressed in bars) represents the necessary pressure a gas (or its partial pressure) must achieve to reach a concentration of unity in the water. The solubility represents the ratios of concentrations between the water phase and the gas phase for a given thermodynamic equilibrium. It is expressed in $mol/m^3/mol/m^3$ in Table 2. Following the ideal gas law, the solubility coefficients do not change with absolute pressure, whereas a correction term must be added in the case of non-ideal solutions.

The solubility of noble gases between gas and liquid hydrocarbon phases is less well constrained, as it is dependent on the oil composition, which may be variable. Two sets of solubility coefficients have been obtained by Kharaka and Specht (1988), for a light oil (API of 34) and an heavy oil (API of 25). The solubility of noble gases between oil and water can be calculated by combining the solubilities between water and gas, and between gas and oil. The result is shown in Figure 2 where the solubilities of the noble gases (in $mol/m^3/mol/m^3$) between a light oil and water are plotted as a function of temperature. For all the noble gases in the range of temperatures presented Figure 2, oil always has higher noble gas concentrations than the associated water, indicating that noble gases are more soluble in oil than in water.

It is important to note that the oil considerably enriches the heavy noble gases (mainly Xe and Kr) relative to water for temperatures between 50 and 90°C. Figure 3 shows noble gas solubilities between different phases at 50°C, highlighting the fractionation that occurs between gas and oil, favoring heavy noble gases in oil and light ones in gases.

As the initial water may be considered to be ASW, the mass balance of the noble gases between phases will follow simple rules, assuming that the initial water was equilibrated with a gas phase, with an oil phase or with both oil and gas phases. Defining H as the ratio of the volume of oil versus the volume of equilibrated water, and G the ratio of the volume of gas versus the volume of equilibrated water, we may write:

$$C_{ASW} = C_W + H.C_H + G.C_G \quad (1)$$

C_H and C_G are calculated versus C_W as:

$$C_H = C_W \text{ solub (oil/water)} \quad (2)$$

$$C_G = C_W \text{ solub (gas/water)} \quad (3)$$

(where solub (x/y) is the solubility of the gas in phase x divided by that in y) It is possible to calculate, for a given amount of oil, water and gas, the noble gas concentrations in each phase, at equilibrium by writing:

$$C_W = C_{ASW}/(1+H \text{ solub(oil/water)} +G \text{ solub (gas/water)} \quad (4)$$
$$C_H = C_W \text{ solub(oil/water)} \quad (5)$$
$$C_G = C_W \text{ solub (gas/water)} \quad (6)$$

An example of the concentration patterns expected is presented in Figure 4, where the volumetric oil/water and gas/water ratios have been taken at 0.1 m^3/m^3 with an oil gravity of 34° API. The figure shows that the gas phase is enriched in all noble gases versus ASW, with an increasing enrichment for the light noble gas fraction. The oil phase is depleted in light noble gases but enriched in krypton and xenon versus ASW. The water equilibrated with these

two phases has lower concentrations than pristine ASW, significantly so for the light noble gases.

This exchange of noble gases between 3 different phases (oil, gas and water) potentially presents complex behavior when temperature is taken into account. Figure 5 represents a plot of two ratios of fossil noble gases $^{36}Ar/^{20}Ne$ versus $^{84}Kr/^{20}Ne$. The three trends shown on the figure correspond to the equilibrium of the three phases, with the temperature of equilibration ranging from 0 to 230 °C. The trend for the oil phase is more variable in the diagram, whereas the gas and water trends present a smaller excursion of these two ratios.

Adsorption/desorption of noble gases on the surface of solids

The physical sorption of noble gases (as no chemisorption may be envisioned in geological environments with these inert gases) on the surface of solid matter (mineral and organic) may be considered as a particular type of phase change, as described previously. However, the formalism that one may use to describe this process is linked to isothermal adsorption curves. Unfortunately, little experimental data is available on the adsorption properties of noble gases on natural minerals and organic surfaces for geological conditions. Several studies were published in the sixties through the eighties on krypton and xenon, as it was observed that these two elements had anomalously low concentrations in the terrestrial atmosphere compared to meteorites. Fanale & Cannon (1971) provide some Langmuir adsorption isotherms for krypton and xenon adsorbed on shale and volcanic ash surfaces. However, the importance of adsorption on the organic matter has been only primarily discussed with respect to reduced carbon fractions of meteorites (Yang et al., 1982; Wacker et al., 1985; Wacker, 1989). Frick and Chang (1977) further presented results of adsorption on kerogens and shales, and indicated that the preferential adsorption of xenon, and to a lesser degree krypton, is higher for kerogens than for shales. Figure 6 presents the analyzed concentrations of noble gases measured in kerogens and shales (Frick and Chang, 1977) compared to air and ASW concentrations. It appears that kerogens fractionate the heavy noble gases from light noble gases. However, their absolute concentrations are lower than in shales and water, meaning that their influence on the noble gas mass balance is smaller. The shales may also present highly fractionated light/heavy noble concentrations, whereas ASW, only controlled by noble gas solubilities, is comparatively less fractionated.
Other constraints on these processes have been obtained through geological case studies. Torgersen and Kennedy (1999) and Zhou et al. (2005) clearly show the importance of adsorption of heavy noble gases (Krypton and Xenon) in geological processes. Torgersen and Kennedy (1999), studying the Elk Hills oil field, USA, show enrichment of Xe/Ar and Kr/Ar relative to air of 576 and 58 times respectively, interpreted as due to preferential adsorption of these on organic-rich shales of the petroleum system. Zhou et al. (2005), studying gases collected in coalbed methane accumulations of the San Juan Basin, USA, also find considerable enrichments of Krypton and Xenon (31 and 146 relatively to ^{36}Ar respectively). These heavy noble gas enrichments are interpreted as due to preferential adsorption on coal macerals. This demonstrates the importance of heavy noble gas adsorption in sedimentary rocks, when severe fractionation is observed between light and heavy noble gases, as was originally suggested by Podosek et al. (1982).

Diffusion in liquids or in gas phases

The fractionation of noble gases between fluid phases (water, oil, gas, supercritical fluids) and during adsorption processes (on mineral and organic surfaces) has been considered so far in the context of thermodynamic equilibrium. The noble gas distribution between rocks and fluids is heterogeneous, implying that equilibrium is not always achieved, and that kinetic processes could affect their concentrations. As pure Darcy flow of a single fluid will not fractionate dissolved species, only diffusion can affect dynamically the absolute and relative concentrations of noble gases. The diffusion coefficients of noble gas are well constrained in pure water (Jähne et al., 1987) and in gases (Reid et al., 1977). Figure 7 summarizes the diffusion coefficients of noble gas in water versus their solubility. Other gas compounds (N_2, CH_4, CO_2, H_2) are added for comparison (Reid et al., 1977). In the oil phase, of course these coefficients depend on the oil composition (viscosity, density, etc...). Modeling the diffusion process in porous rocks is intricate as the geometry and petrography of the matrix will significantly alter the effective diffusion coefficients (Rebour et al., 1997). A slowing down effect always occurrs during transport of dissolved gases in porous matrices, due to the reduction of porosity (the noble gases will mainly diffuse in fluid phases filling the porosity), the tortuosity and the permeability of the rocks. These parameters should decrease the effective diffusion coefficients by a constant parameter for all gases. However, it has been noticed (Giannesini, 2008. Magnier et al., 2011) that this diffusivity reduction is not the same for the whole series of noble gas compounds, with a larger flux reduction for the heavier noble gases. This is interpreted as due to the preferential adsorption of the heavy noble gases on the surfaces of minerals and organic compounds present in the sedimentary rocks, adding a chromatographic effect to the simple fluid phase diffusion process. A quantification of this relative retention has been hypothesized to depend on the mineralogy of the rocks and its clay content.

Considering gas diffusion through a simple membrane as an analog to a thin sedimentary layer, the flux of each gas should be proportional to the product of the diffusion coefficient in the membrane and the solubility of the species in the membrane (Crank, 1975, here multiplied by the porosity filled with water). For the noble gases, this product is not monotonous, but presents a minimum for neon (Figure 8). Even if helium is generally considered to be the most mobile noble gas, it can be seen that, in a water membrane, it is not systematically the most mobile. However, considering krypton and xenon adsorption (see previous paragraph and Torgersen and Kennedy, 1999; Zhou et al., 2005), this order has to be revised in porous rocks, and generally, a decrease in mobility is indeed correlated with noble gas atomic mass (Magnier et al., 2011). In conclusion, it seems difficult to isolate pure single phase diffusion in sedimentary rocks, as the migration processes always involve a complex combination of physical processes, including advection, water diffusion and adsorption.

A.3- The atmospheric noble gas isotopes: a possible mass balance between water, oil and gas phases

It has been shown that one of the main reservoirs of noble gas isotopes interacting with a petroleum system is ASW. All the atmospheric noble gases are dissolved in the aquifer waters, implying that their original concentrations are known, as their atmospheric concentration and solubility coefficients are well constrained. Some noble gas isotopes there are sourced uniquely from ASW, being unradiogenic and with sufficiently low mantle concentrations (compared to ASW) to be neglected; notably ^{20}Ne, ^{36}Ar, ^{84}Kr and ^{132}Xe can be considered to be ASW-derived. Therefore, from their concentrations in aquifers, their measured concentrations in a hydrocarbon phase are consequently related to the amount of aquifer water exchanged with the hydrocarbon phase: no interaction at all would imply zero

concentrations in the hydrocarbon phase (which is never seen), whereas high oil/water ratios would feed the hydrocarbon phase with high concentrations of these isotopes. Several papers have already demonstrated the geological interest in these fossil interactions recorded by the noble gas isotopes. With well known initial concentrations and physical properties, exchanges between oil, gas and water phases can readily be traced: Ballentine et al. (1991) investigated noble gas partitioning in the Pannonian Basin, Ballentine et al. (1996) in The Magnus Opus field, with direct measurements of noble gas concentrations in the oil phase, Battani et al. (2000) for the giant gas fields of the Indus Basin, and Prinzhofer et al. (2000) for the gas accumulations of the Mascupana Basin, Mexico.
The basis for all these studies is that it is possible to calculate a Hydrocarbon Gas (G)/Water (W) equilibrium ratio by combining the solubility equation with mass balance equations:

$$G/W = C_{ASW}/C_g - \beta \quad (7)$$

With G/W as the Gas/Water ratio, C_{ASW} the concentration of the noble gas isotope in the Air Saturated Water, C_g the concentration in the gas phase, and β the solubility of the isotope in water.

However, this calculated Gas (G) /Water (W) ratio may be different depending on the gas used (neon, argon, krypton or xenon). The reason is that a thermodynamic equilibrium is assumed between the two phases, which is rarely the case in sedimentary basins for all the noble gases from helium to xenon. Figure 9 shows that the calculated G.W ratios obtained using ^{36}Ar and ^{84}Kr give the most consistent results, for G/W ratios ranging from 0.2 and 200 m^3/m^3, i.e. three orders of magnitude. The calculated G/W ratios (using ^{20}Ne, ^{36}Ar and ^{84}Kr) appears, for some systems, to be larger for heavier noble gas compounds, whereas for some other petroleum systems, the opposite is observed (Figure 10). These contrasting behaviors may possibly be interpreted as due to different time scales for the age of accumulation and the age of preservation of the hydrocarbon accumulations. Considering the higher mobility of lighter noble gases, a lack of equilibrium between the accumulating hydrocarbon phase and water would imply larger gas/water ratios for the heavy noble gases, whereas partial gas leakage out of the accumulation would favor the opposite, i.e. larger Gas/Water ratios for the light noble gas compounds. It is interesting to note that for more recent accumulations the dominant process is an absence of equilibration between hydrocarbon and water, whereas for older geological systems, the dominant factor seems to be loss from the hydrocarbon reservoirs.

Another example of using noble gases to calculate Gas/Water ratios is presented Figure 11. The gas samples were collected from the Trinidad Islands (Trinidad and Tobago), some (in red) were sampled from oil accumulations, at producing well heads. The gases were collected at the separator, and correspond to the gas in solution in oil at the depth of the geological reservoir. Other samples (in green) were sampled from mud volcanoes. These settings are quite different: the latter correspond to eruptions of mud and hydrocarbon gas from undercompacted layers of the source rocks from which the oil accumulations are derived. This phenomenon is particularly useful as it allows mud and migrating gas to be directly sampled from the “kitchen” of the petroleum system (Battani et al., 2011). Calculating the associated gas/water ratios in these samples, it is clear that all the gases associated with oils present higher gas/water ratios (i.e. less water interaction with the hydrocarbons) compared to gases seeping from mud volcanoes. The association of a gas phase with water and mud, emitted at the same time, can explain the larger exchange with water than for gas compounds dissolved

in the oil. Furthermore, gas/water ratios measured on the samples presented consistent quantitative values irrespective of the ASW derived noble gas used (^{20}Ne, ^{36}Ar or ^{84}Kr), indicating good equilibrium between the water and gas phase was reached. The gas/water ratios for the gas associated with oil and sampled from the geological reservoir were estimated to be between 10 and 100 m^3/m^3, whereas gases sampled from mud volcanoes had gas/water ratios between 1 and 10 m^3/m^3.

Figure 12 illustrates a correlation between the carbon isotopic ratio of methane dissolved in oil accumulations, which is sensitive to the extent of bacterial degradation, and the gas/water ratios calculated using ^{84}Kr. Gases that have the lowest gas/water ratios (i.e. most water interaction) have more negative $\delta^{13}C$ of methane, indicating an increasing contribution of bacterial methanogenesis. As the bacterial activity is highest at the water interface, an increase of the bacterial activity is consistent with an increase in water-oil interaction. The quantification of the proportion of water required for a given amount of biodegradation is thus possible using noble gas derived Gas/Water ratios.

A.4- Radiogenic noble gas isotopes : qualitative or quantitative estimates of geological residence times of fluids in the subsurface

The two most commonly used radiogenic noble gas isotopes in oil and gas exploration are ^{4}He and ^{40}Ar. ^{4}He comes from the natural radioactive decay of ^{235}U, ^{238}U and ^{232}Th, whereas ^{40}Ar is generated through the radioactive decay of ^{40}K. Considering that the ^{40}Ar/^{36}Ar of the atmosphere has a value of 298.6, one may calculate the additional radiogenic ^{40}Ar (commonly known as ^{40}Ar*):

$$^{40}Ar^* = {}^{40}Ar - 298.6\ {}^{36}Ar \qquad (8)$$

The amount of ^{40}Ar* is a function of the average potassium content of the rocks interacting with the fluid, the proportion of fluid versus rocks (related to the average porosity as $\Phi/(1-\Phi)$. Steiger and Jager (1977) calculated the production of ^{40}Ar* per year and per cubic centimeter (cm^3) of rock as:

$$^{40}Ar^* = 1.05\ 10^{-17}(K)\ cm^3\ STP\ cm^{-3}\ y^{-1} \qquad (9)$$

With an average ^{40}K concentration of 28000 ppm, we may calculate:

$$^{40}Ar^* = 2.94\ 10^{-13}\ cm^3\ STP\ cm^{-3}\ y^{-1} \qquad (10)$$

The amount of ^{36}Ar, considered as only sourced from ASW, is a function of the concentration of ASW and of the average porosity Φ of the rocks. It is then possible to assess a model age for a crustal fluid related to the ratio ^{40}Ar*/^{36}Ar:

$$T(y) = \frac{C_{ASW}^{^{36}Ar}\ (cc\ STP/cc)}{2.94\ 10^{-13}} \frac{\Phi}{(1-\Phi)} \frac{^{40}Ar^*}{^{36}Ar} \qquad (11)$$

The same kind of calculation may be done for the generation of ^{4}He, also associated with ^{36}Ar, as the second isotope of helium cannot be considered as a fossil isotope (due to nuclear

and possible mantle fluid contributions). Steiger and Jager (1977) calculated the amount of radiogenic ^{4}He generated in rocks:

$$^4He = 1.207*10^{-13}[U] + 2.867*10^{-14}[Th] \ cm^3 \ STPg^{-1}y^{-1} \quad (12)$$

From the average crustal concentration of uranium and thorium, the same kind of formula as shown above may give a model age using ^{4}He and ^{36}Ar:

$$T(y) = \frac{C^{^{36}Ar}_{ASW} \ (cc \ STP/cc)}{1.74 \ 10^{-12}} \ \frac{\Phi}{(1-\Phi)} \ \frac{^4He}{^{36}Ar} \quad (13)$$

It must be stressed that this kind of modeling implicitly implies a closed system, in relation to the radioactive/radiogenic compounds. As we deal with highly mobile gases such as helium and argon, it is clear that these age calculations should be used with extreme care, as external fluxes of 4He and 40Ar (Zartman and Wasserburg, 1961; Sano et al., 1986; Ballentine and Sherwood-Lollar, 2002), as well as differential loss of these (Pinti and Marty, 1995; Prinzhofer et al., 2010) are common features in geological basins

Mud volcanoes from the Makran area (Pakistan)

The migration of radiogenic isotopes in fluids within porosity, generated by the constitutive rock minerals , has been studied by several authors (Mamyrin and Tolstikhin, 1984; Elliot et al., 1993; Ballentine and Burnard, 2002). They consider that the rate of release of ^{4}He, as an alpha particle, mobile and with an important initial energy, occurs more easily and at lower temperature than ^{40}Ar, bigger atom and residue of ^{40}K, which needs more energy, i.e. higher temperature in order to enter the fluids within the porosity. Furthermore, it has been suggested that bacterial gas generation may be distinguished from thermogenic generation using these tracers, in part because their generation temperature are quite different (Elliot et al., 1993). As an illustration, Figure 13 presents geochemical data obtained from mud volcanoes from Makran (Pakistan; Ellouz-Zimmermann et al., 2007). These impressive natural structures (sometimes more than 1000m high), are composed of mud and gas expelled from under compacted sediments (Deville et al., 2003). Figure 13a shows the carbon isotopic ratios of methane and carbon dioxide (the two main gas compounds of these mud volcano gases). These gases have either heavy methane and CO_2 $\delta^{13}C$ (red circles), indicating a thermogenic origin for methane and a mineral origin for CO_2 (possible through high temperatures) or else the carbon isotope ratio of methane is in the range of bacterial generation and is associated with light $\delta^{13}C$ of CO_2 of biological origin (green squares).
Combining the data with noble gas isotope analyses (Figure 13b), the two gas "families" appear significantly different. The ^{4}He/^{40}Ar* ratios are higher for bacterial gases, explained by the fact that at low temperatures ^{40}Ar is expelled less easily that ^{4}He from the parent mineral lattice. The concentrations of ASW noble gas isotopes coming from the aquifer, ^{136}Xe in this example, shows that the bacterial gas underwent more interaction with the nearby aquifer water than the thermogenic gas. This can be seen by lower $1/^{136}$Xe, i.e. higher concentrations of ASW noble gas isotopes, associated with a higher Water/Gas ratio.

Radiogenic noble gas isotope ratios also allow an accumulation or exchange period to be tentatively calculated for given gas accumulations, provided the average porosity of the sedimentary system is known (here, the mud of the undercompacted sediments producing the

mud volcanoes), assessed using a slightly different formalism by Zhou and Ballentine (2006). Normalizing the concentrations of two radiogenic isotopes (^{4}He or $^{40}Ar^{*}$) to an ASW isotope (here ^{36}Ar), the ratio radiogenic/ASW is then a function of both porosity and time. Assuming an average porosity of 15% for Makran, Figure 14 then shows the correlation between the model ages calculated using $^{4}He/^{36}Ar$ and $^{40}Ar/^{36}Ar$. It appears that for all the samples, the calculated age involving helium is younger than that with argon. This may in part be explained by a higher mobility of helium compared to argon and the fact that the memory of argon is probably more significant, rendering a better estimate of the hydrocarbon age with argon. The second observation from the model age is that all thermogenic gases present older ages than bacterial ones, irrespective of the chronological system used (for the $^{40}Ar/^{36}Ar$ dating system, the retention of ^{40}Ar in the minerals associated with the bacterial gases could be an alternate explanation of these age differences, as discussed above and in the review of Ballentine and Burnard, 2002). This is also consistent with a deeper, older origin of the thermogenic gases compared to the more superficial and probably more recent origin of the bacterial gases of the eastern Makran region.

Oil and gas accumulation in a Paleozoic Basin, Brazil

Prinzhofer & Battani (2003) presented a case study on a Paleozoic Brazilian basin, consisting of two adjacent anticlinal structures filled with oil and gas. The ratios $^{40}Ar^{*}/^{36}Ar$ of each of these structures are quite consistent: the concentrations of $^{40}Ar^{*}$ and ^{36}Ar make an independent positive correlation for each structure, with a correlation line intercepting the origin, and a difference in slope of about 30% between the two accumulations (Figure 15). The differences in $^{40}Ar^{*}/^{36}Ar$ may be interpreted as a difference in hydrocarbon residence times within the two structures. Indeed, it is likely that both isotopes exchange between the hydrocarbon phase and the other phases of the petroleum system (water, minerals). ^{36}Ar originates only from ASW and may be considered as an internal normalization for $^{40}Ar^{*}$, whose absolute amount is directly linked to the average residence time of the fluid (assuming that the concentrations of potassium and the porosity of the rocks are similar for both hydrocarbon accumulations, which has been confirmed by geological studies of this area). The fact that hydrocarbon fluids with the greatest residence times (fields C and D) are less mature than the others (fields A and B) corroborates the longer accumulation time. Moreover, this interpretation is in agreement with the more efficiently accumulated fluids generating more mature hydrocarbons (Figure 16).

B- Sources of non hydrocarbon gases (He, CO_2, N_2)

One of the most commonly used application of noble gas geochemistry in oil and gas exploration is to quantify the origins of non hydrocarbon gas compounds present in accumulations. N_2 and CO_2 are regarded of paramount importance as their presence in large proportions in hydrocarbons reservoirs changes the reservoir's commercial value. Negative properties are also associated with CO_2, as it is known to acidify water, requiring the use of special well tubing for hydrocarbon production. Moreover, removal of CO_2 implies its subsequent elimination, with all the operational, financial and societal concerns involved (Carbon Capture and Sequestration). Another unwelcome non-hydrocarbon gas sometimes in significant quantities is H_2S. Nonetheless this compound is generally autochthonous, generated within oil and gas accumulations (its high reactivity prevents its migration), and it has not been studied using the noble gases to date (as these generally provide information on fluids migrating into a hydrocarbon accumulation). Among non-hydrocarbon gases associated

with hydrocarbons, helium may be sometimes present in amounts large enough to become economically interesting. The geology and interest of helium will be discussed later.

It has been recognized for many years that some hydrocarbon accumulations present a substantial contribution of mantle noble gas (Oxburgh et al., 1986; Ballentine et al., 1991). The best indicator of mantle fluid contribution has been and remains the helium isotopic ratio, $^3He/^4He$. However, addition of radiogenic ^4He may reduce the isotopic ratio and effectively mask the presence of mantle fluids. Alternative diagrams have recently been suggested, solely using the ^3He concentration in the hydrocarbon phase, or using the ratio $CO_2/^3He$ (Sherwood-Lollar et al., 1997; Ballentine et al., 2002). According to these authors, a magmatic fluid would present a $CO_2/^3He$ ratio between 10^9 and 10^{10}. Any value above this range would suggest that there was no direct mantle contribution, whereas values below this range would correspond to more complex signatures such as partial loss of mantle CO_2. A Brazilian Paleozoic basin rich in evaporites (halite and anhydrite) has $CO_2/^3He$ lower than the mantle value (Prinzhofer and Battani, 2003), as can be seen Figure 17a, which could be interpreted as production of ^3He via nucleogenic reactions. Figure 17b shows the same gases in a $^{40}Ar/^{36}Ar$ versus R/Ra diagram. For mantle and radiogenic Ar contributions, the $^{40}Ar/^{36}Ar$ should increase. But in the case of a mantle contribution, this increase should correlate positively with $^3He/^4He$ (expressed as R/Ra) as the mantle value is around 8 Ra, whereas in the case of a radiogenic contribution, the increase of ^4He would decrease $^3He/^4He$. This is what is observed on Figure 17b, indicating that there is no evidence for a mantle contribution. The excellent correlation between the two isotopes ^3He and ^4He (Figure 17c) favors a common origin.

The origin of CO_2 may be characterized using its carbon isotopic ratios (Figure 18). A low $\delta^{13}C$ value generally indicates an organic carbon origin, whereas a positive (heavy) $\delta^{13}C$ isotopic value is generally associated with oil biodegradation. $\delta^{13}C$ values around -4 per mil are generally linked to a mineral origin of the CO_2, particularly for high proportions of CO_2 (Figure 18, and Jenden et al., 1993). The two possible origins of mineral CO_2, carbonate decomposition and mantle fluids, cannot be distinguished with carbon isotope ratios alone. The associated noble gases are often used to test the presence of a mantle fluid invading the petroleum system. Figure 19 shows that the gas samples corresponding to high CO_2 concentrations and $\delta^{13}C$ values around -4 ‰ PDB are clearly associated, in this database, to a large mantle contribution, visible with the helium isotopic ratios.

In order to better assess this mantle contribution, a correlation between the isotopic ratios of helium and argon (Figure 20) shows that two main trends can be identified. A trend with a negative slope, similar to the trend of Figure 17b, corresponds to addition of radiogenic ^4He and ^{40}Ar, and is related to the natural radioactivity of the sediments and possibly the underlying continental basement. A positive slope corresponds to a mixture with a mantle end-member.

Other mixing diagrams can be used to distinguish different physical processes. For instance, $^{20}Ne/^4He$ versus R/Ra is used to plot various sources of noble gases, notably the atmosphere and ASW, the mantle end-member and a crustal/radiogenic end-member (Figure 21). It should be mentioned that the crustal end-member must contain a certain amount of ^3He, as a pure ^4He helium end-member would not explain a large portion of the gas samples, which would have too low $^{20}Ne/^4He$ for a given R/Ra. The radiogenic endmember needs to be around 0.02 Ra, demonstrating that traces of ^3He in gas accumulations may be of purely nucleogenic origin. In such a diagram, it is possible to quantify the proportions of ASW,

mantle and crustal sources (considering that the atmospheric component is not present in non air-contaminated samples) for each gas sample.

The neon isotopes may also be used to characterize various sources of a gas accumulation. Figure 22 presents data from Gilfillan et al. (2009) from gas accumulations in the United States composed dominantly of CO_2. Plotting the data in a $^{20}Ne/^{22}Ne$ versus $^{21}Ne/^{22}Ne$, the three end-members mantle, ASW and crustal nucleogenic sources may be clearly indentified. The dataset shows that, depending on the gas province, there are variable contributions from each end-member, with a poorly defined end-member possibly corresponding to the crustal basement, located in the middle of the mixing surface. In this area, three distinct trends may be distinguished, joining the central end-member to each of the well documented trends, i.e. the mantle, the aquifers and the radiogenic poles (see Chapter 8 of this volume).

An important and not completely resolved question remains: having demonstrated that mantle fluids can contribute to petroleum systems and other gas accumulations, how then do these mantle fluids migrate from their source (the mantle) into the sedimentary sequences? If volcanism is present in the surrounding rocks, this may be the principal carrier of mantle fluids. However, in most cases mantle fluids are present in sedimentary basins free of local volcanic rocks. Furthermore, a mantle fluid will introduce not only helium but also lower concentrations of heavier noble gases (neon, argon, xenon), possibly overprinted in some cases with ASW contributions, and significant quantities of CO_2. Diffusion cannot be the only migrating process, as the time needed for diffusion through the entire continental crust is too long. Therefore a fluid flux in a constituted phase (supercritical?) is implied. As the porosity of the basement is much too low to permit Darcy, fractures have to be envisioned to allow these fluids to rise through sedimentary reservoirs. Hydraulic fracturing due to the occurrence of supercritical mixture of mantle related CO_2 and H_2O explains large contributions of mantle fluids in metasomatic ore deposits (see Chapter 11 of this volume). The discovery of mantle lead associated with asphaltenes in the Potiguar Basin (Brazil, Dreyfus, 2006), in which mantle helium is also found (Prinzhofer et al., 2010) confirms the metasomatic introduction of mantle fluids through hydraulic fracturing.

C-Control on migration processes

It is easy to imagine that helium is more mobile than other gases. In fact, the differential migration efficiency of noble gases may be studied and used for tracing hydrocarbon migration through sedimentary rocks.
The noble gases, being inert chemically, are not affected by chemical or biological processes, precluding complications of mixing chemical and physical processes, as occurs for the carbon isotopic ratio of methane for example. As a result, distinguishing source and migration effects on stable isotope ratios is not always straightforward (Prinzhofer and Pernaton, 1997), whereas the noble gas ratios are only affected by physical processes, linked to migration. From the ASW noble gas isotopes, ^{20}Ne, ^{36}Ar, ^{84}Kr or ^{132}Xe, interaction with water that was at equilibrium with the atmosphere (ASW) can be demonstrated. Air itself should not be a significant part of the fluid as there is no direct interaction between deep hydrocarbon fluids and the atmosphere, except in the case of an accidental contamination during gas sampling. Figure 23 presents $^{84}Kr/^{20}Ne$ versus $^{36}Ar/^{20}Ne$ correlations for a database of various oil and gas fields around the world. Figure 24 presents in the same diagram the CO_2-rich accumulations of Colorado, USA (data from Gilfillan *et al.*, 2009). The ratios share the same denominator, therefore a mixing trend between two end-members should plot on a straight

line: in a mixture of ASW and the atmosphere, any sample in thermodynamic equilibrium with the surrounding rocks should plot on a straight line joining the ASW – air compositions. From Figures 23 and 24 this is not the case, and the oil and gas samples plot on a curve passing though the atmospheric end-member, but not through the ASW point (whereas these samples can be demonstrated not to be contaminated by any air contribution during their sampling). Furthermore, these natural samples present a fractionation trend extending to a much larger range than that limited by their possible sources. Contributions from other sources (mantle, organic matter) can be excluded as their absolute concentrations are too small to significantly affect the data. This demonstrates that the noble gases have been fractionated, and that they are not in equilibrium with the surrounding rocks and fluids. As previously presented, only three physical processes may explain these trends: Exchange between phases, diffusion and adsorption. These three processes are linked to the migration of the fluids through the porous rocks, without reaching thermodynamic equilibrium.

In order to interpret and integrate these observations in a more quantitative model of fluid migration, migration experiments have been performed using CO_2, CH_4 or N_2 as the main constituent of the gas phase, with added traces of noble gases (Giannesini, 2008. Magnier et al., 2011, Vacquand *et al.*, 2011). As described in the paragraph devoted to noble gas diffusion, the flux of noble gases in porous rocks is controlled not only by water diffusion, but also by adsorption/desorption of noble gases on mineral surfaces. This last process is largely negligible for helium and neon, but of primordial importance for the heavier noble gases (Ar, Kr, Xe). Combining these experimental results with the observation of natural gas fractionation in Figures 23-24, it should then be possible to use noble gas isotopes in order to quantify migration processes affecting hydrocarbon fluids (oil and gas). The models need then to be assessed at different geometric and temporal scales: geological times, at the basin scale and at the reservoir scale, or human timescales for hydrocarbon migration during oil and gas extraction.

D-Controls on oil and gas production

A new and challenging interest for noble gas geochemistry applied to the oil and gas industry is linked to a better assessment of hydrocarbon production. In fact, one of the big challenges for this century is changing oil and gas resources into reserves, i.e. making production of identified hydrocarbons feasible technically and economically. This concerns both conventional reservoirs (accumulations in sedimentary structures with high permeability) and unconventional reservoirs (rocks with low permeability, such as gas and oil shales, and heavy/viscous oils). The associated porosity is not generally limiting, as porosity controls only the amount of trapped fluids, and not its mobility during extraction. Two series of questions are raised with these issues:

- characterization of the heterogeneity of the reservoir, in terms of permeability barriers, hydrocarbon saturation, fluid communication between wells, and the 3D image of the producing area,
- monitoring production, or in other terms, at what stage of production is the reservoir? What is the proportion of currently extracted hydrocarbons versus the total extractable hydrocarbons accumulated in a given structure? What is the relative saturation in gas and in water for a gas shale system, etc…?

Noble gas isotopes, as tracers of physical processes, insensitive to chemical effects, are potentially excellent tracers for these tasks, even if this new application of noble gases is still not yet fully developed. Nevertheless, it has been demonstrated in earlier paragraphs that the hydrocarbon/water ratio can be quantitatively calculated, and which may be used at the reservoir scale. Additionally, the composition of noble gas in hydrocarbons may vary over several orders of magnitude for both their concentrations and isotopic ratios. Potential heterogeneities may thus be investigated with higher precision using noble gases, as the key parameter for a sensitivity study is the ratio between the range of variation and the accuracy of the measurement. For example, the precision for a $\delta^{13}C$ measurement is about 0.5 per mil, whereas the usual variation of $\delta^{13}C$ for methane in a reservoir is around 30 delta units, and less than 5 delta units for the C2+ fraction. This gives a selectivity parameter for methane heterogeneity of 60 (30/0.5) and 10 for the C2 fractions. For the associated helium concentrations, the variations may be from 100 to 2,000 ppm, with an accuracy of about 3% for the concentration measurement. The resolution between samples is estimated at 120. This overall accuracy is consequently the same for all other noble gas parameters (concentrations and isotopic ratios), increasing significantly the potential to identify or characterize a fluid heterogeneity within a petroleum reservoir, indicative of a lack of mixing in the reservoir. This greater sensitivity to heterogeneities, associated with the fact that the noble gas compounds are only sensitive to physical processes, results in a promising potential for future noble gas applications in oil and gas production, when the usual techniques of production monitoring (geophysics, organic geochemistry) are insufficiently sensitive to provide accurate predictions.

E-Helium as an important natural resource

The only source of helium for humankind is associated with natural gas accumulations, as the atmospheric concentration of helium is only 5ppm, whereas sustainable helium production requires around 3000ppm He. Helium is one of the natural products with the most significant increases in demand (with a price increase of around 25% for the year 2009). The main applications for helium are cryogenic uses (32%), pressuring and purging (18%), inert atmospheres for electronic equipments (18%), welding (13%) , leak detection (4%), breathing mixtures (2%) and other applications (13%). In some applications, other inert gases could be used, although not for all. Other potential uses of He could become significant if helium reserves were increased accordingly: inflated balloons for ore transportation in countries without road or railways infrastructures (center of Africa for example), heat carrier gas for new generations of nuclear plants, etc... However, the reserves of helium today (about 8.5 billions of cubic meters) are relatively restricted, and represent about 25 years of production based on present consumption. However, it is important to take into consideration that reserves are calculated solely for the three helium producers at present, i.e. USA, Russia and Algeria. Qatar is building a new helium plant for the biggest gas field on Earth, the North Field. This new plant is expected to supply 25% of the world production by 2013. The North Field is poorer in helium concentration than the 0.3% considered today as the cut off value. The Liquefied Natural Gas (LNG) plants which already exist in Qatar allow extraction of commercial concentrations of helium, which appears with the residual non-liquefied part of the natural gas. This first concentration step by gas liquefaction produces a residual gas whose helium concentration is higher than the required 0.3% cut off value.

More recently, sources of commercial helium have been generated from LNG plants, often located in countries rich in large gas fields. The residual gas (that which cannot be liquefied)

in fact concentrates all the helium, as this gas is one of the most difficult to liquefy. Considering the small proportion this residue represents, the helium concentrations become sufficiently large to overcome the cut-off value of 0.3% in a lot of cases, even if the "geological" helium concentration is much smaller (a value of 0.05% is considered as the pre-LNG cut-off limit). Qatar becomes one the most important country for helium reserves, as they have already built several LNG plants. This new He production method will certainly change the economics of helium trading, as the market will be more international (for the moment, the USA is the major exporter of helium by far), and reserves will grow drastically. It is however still important to analyze helium concentrations in any gas field discovery, as this gas is not so commonly quantified (problems of sampling quality, as well as the common use of helium as the carrier gas of the gas chromatographic system which quantify the gas compositions).

It is important to note that if today, the reserves of helium are very small, no systematic exploration of this gas has been undertaken yet, meaning that most of the naturally occurring helium fields may be considered as undiscovered (or more precisely, some large gas fields have not been estimated so far for their helium potential).

Geologically speaking, the occurrence of relatively high He concentrations has been difficult to explain. The best known He gas field is the large Hugoton-Panhandle gas field of Texas (Gold and Held, 1987; Ballentine and Sherwood Lollar, 2002). In this field, it seems that the absolute amount of helium cannot be explained by helium generated in situ in the basin sediments, as their U + Th concentrations cannot generate the radiogenic ^4He accumulated in the reservoir (Ballentine and Sherwood Lollar, 2002). This means that an extra-basinal source of helium needs to be assessed. The crustal basement seems a good candidate, as it is composed of U and Th-rich acid metamorphic and plutonic rocks. However, the transfer mechanism has remained problematic. The fact that helium-rich gas fields are accompanied by non hydrocarbon gas compounds, either N_2 or CO_2, may provide the explanation to helium migration; these non hydrocarbon gases are considered to be generated in metamorphic areas generating nitrogen (Palya et al., 2011), from high temperature decarbonation of carbonates or mantle hydrothermal fluids for CO_2. In all these cases, these extra-sedimentary fluids cross basement rocks before reaching the sedimentary basins, ending up in the gas traps. Mantle fluids were discussed in the paragraph devoted to non hydrocarbon gases and migrate from the mantle to the sedimentary basins probably via hydraulic fracturing. It is fairly clear that during their migration, mantle fluids will interact with the rocks in the continental crust located between the mantle formations and the sediments. It may then be considered that these supercritical fluids (CO_2, H_2O, N_2) act as carrier gases for helium, which had been generated in the plutonic rocks of the basement, finishing in the sedimentary trapping systems. This would well explain the excellent correlation observed between nitrogen, helium, neon concentrations as well as nitrogen isotopic ratios in the Hugoton-Panhandle accumulations for example (Figure 25, from Brown, 2010): as for the ratio He/N_2 it may be linked to the specific leaching of the basement, the absolute concentrations related to the dynamics of N_2metamorphism, and to the radiogenic production of helium in the continental rocks. However, some authors explain, through migration modeling, high helium concentrations gas fields without contributions from extra-basinal fluids (Brown, 2010), meaning that further quantitative studies are needed.

References

Ballentine C.J., O'Nions R.K., Oxburgh E.R., Horvath F. and Deak J. (1991) Rare gas constraints on hydrocarbon accumulation, crustal degassing and groundwater flow in the Pannonian Basin. Earth and Planet. Sci. Lett. 105: 229-246

Ballentine C.J. and O'Nions R.K. (1994) The use of natural He, Ne and Ar isotopes to study hydrocarbon-related fluid provenance, migration and mass balance in sedimentary basins. From Parnell J. (Ed.), 1994, Geofluids: Origin, migration and evolution of fluids in sedimentary basins. Geological Society Special Publication N° 78, pp. 347-361

Ballentine C.J., O'Nions R.K. and Coleman M.L. (1996) A Magnus Opus: Helium, neon and argon isotopes in a North Sea oil field. Geochim. Cosmochim Acta. 60: 831-849

Ballentine C.J. and Burnard P. G. (2002) Production, release and transport of Noble Gases in the continental crust. In "Noble Gases in Geochemistry and Cosmoschemistry", Review in Mineralogy and Geochemistry. 47: 481-538

Ballentine C.J., Burgess R. and Marty B. (2002) Tracing fluid origin, transport and interaction in the crust. In "Noble Gases in Geochemistry and Cosmoschemistry", Review in Mineralogy and Geochemistry. 47: 539-614

Ballentine C.J. and Sherwood Lollar B.S. (2002) Regional groundwater focusing of nitrogen and noble gases into the Hugoton-Panhandle giant gas field, USA. Geochim. Cosmochim. Acta. 66, 14:2483-2497

Ballentine C. J., Marty B., Lollar B. S., and Cassidy M. (2005) Neon isotopes constrain convection and volatile origin in the Earth's mantle. *Nature.* 433, 7021: 33-38

Battani A., Sarda P. and Prinzhofer A. (2000) Basin scale natural gas source, migration and trapping traced by noble gases and major elements ; the Pakistan Indus Basin. Earth and Planet. Sci. Lett. 181: 229-249

Battani A., Prinzhofer A., Deville E. and Ballentine C.J. (2011) Trinidad Mud Volcanoes: The Origin of the Gas. in L. Wood, ed., Mobile shale basins: AAPG Memoir 93, pp. 1 – 14

Berecz E. and Balla-Achs M. (1983) Gas hydrates. English translation of Gazhidratok. Amsterdam : Elsevier, 343 p. ISBN 0444996575 : Series "Studies in inorganic chemistry" N° 4

Bosh A. and Mazor E. (1988) Noble gases association with water and oil as depicted by aztmospheric noble gases: case studies from the southeastern Mediterranean Coastal Plain. Earth and Planet. Sci. Lett. 87: 338-346

Brown A. (2010) Formation of high helium gases: a guide for explorationists; 2010 AAPG Conference, April 11-14, New Oleans, Louisiana, USA

Burnard P.G., Graham D.W. and Farley K.A. (1997) Vesicle-specific noble gas analyses of "popping rocks": implication for primordial noble gases in Earth. Science. 276: 568-571

Crank J. (1975) The mathematics of diffusion, Oxford University Press, Oxford, 424p.

Crovetto R., Fernandez-Prini R. and Japas M.L. (1981) Solubility of intert gases and methane in H2O and in D2O in the temperature range of 300 to 600K. J. Chem. Phys. 76: 1077-1086

Deville E., Battani A., Griboulard R., Guerlais S., Herbin J.P., Houzay J.P., Muller C. and Prinzhofer A. (2003) Mud volcanism origin and processes: New insights from Trinidad. Special publication 216 of the Geological Society (London) on Subsurface Sediment mobilisation, p. 475-490

Dreyfus S. (2006) Impact de la migration et de la biodégradation sur les signatures chimiques et isotopiques des traceurs métalliques dans les huiles. PhD. Pau University/IFP, 27th April 2006

Dunai T.J. and Baur H. (1995) Helium, neon and argon systematics of the European subcontinental mantle: implication for its geochemical evolution. Geochim. Cosmochim. Acta. 59: 2767-2783

Dyadin Y.A., Larionov E.G., Mirinskij D.S., Mikina T.V. and Starostina L.I. (1996) Hydrate formation in the Krypton-Water and Xenon-Water systems up to 10 kbars. 2nd international conference on natural gaz hydrates : (Toulouse, June 2-6, 1996): 59-66

Elliot T., Ballentine C.J., O'Nions R.K. and Ricchiuto T. (1993) Carbon, helium, neon and argon isotopes in a Po Basin (northern Italy) natural gas field. Chemical Geology. 106: 429-440

Ellouz-Zimmermann N., Deville E., Muller C., Lallemant S., Subhani A.B. and Tabreez A.R. (2007) Impact of sedimentation on convergent margin tectonics : Example of the Makran accretionary prism (Pakistan), In Lacombe, O., Lavé, J., Roure, F. and Vergés, J. Eds "Thust Belts and Foreland Basins, from fold kinematics to hydrocarbon systems", Springer-Verlag: 327-350

Fanale F.P. and Cannon W.A. (1971) Adsorption on the Martian regolith. Nature. 230: 502-504

Frick U. and Chang S. (1977) Ancient carbon and noble gas fractionation. Proc. Lunar Sci. Conf 8^{th}: 263-272.

Giannesini, S., Prinzhofer, A., Moreira M. and Magnier, C. (2008) Influence of the bound water on molecular migration of CO_2 and noble gases in clay media. Goldschmidt Conference, Vancouver, Canada.

Gilfillan S.M.V., Sherwood-Lollar B., Holland G., Blagburn D., Stevens S., Schoell M., Cassidy M., Ding Z., Zhou Z., Lacrampe-Couloume and Ballentine C.J. (2009) Solubility trapping in formation water as dominant CO2 sink in natural gas fields. Nature. 458: 614-618

Gold T. and Held M. (1987) Helium-nitrogen-methane systematic in natural gases of Texas and Kansas. Journal of Petroleum Geology. 10 N° 4: 415-424

Graham D.W. (2002) Noble gas isotope geochemistry of mid-oceanic ridge and ocean island basalts: Characterization of mantle source reservoirs. . In "Noble Gases in Geochemistry and Cosmoschemistry", Review in Mineralogy and Geochemistry. 47: 247-304

Harvey A.H. (1998) Applications of Near-Critical Dilute-Solution Thermodynamics. Ind. Eng. Chem. Res.. 37 N° 8: 3080–3088

Honda M., McDougall I., Patterson D.B., Doulgeris A. and Clague D.A. (1991) Possible solar noble-gas component in Hawaiian basalts. Nature 349: 149-151

Jähne B., Heinz G. and Dietrich W (1987) Measurement of the diffusion coefficient of sparingly soluble gases in water. J. Geophys. Res. 92: 10,767-10,776

Jenden P.D., Kaplan I.R., Poreda R.J. and Craig H. (1988) Origin of nitrogen-rich natural gases in the California Great Valley: Evidence from helium, carbon and nitrogen isotope ratios. Geochim. Cosmochim. Acta. 52: 851-861

Jenden P.D., Hilton D.R., Kaplan I.R. *and* Craig H. (1993) Abiogenic Hydrocarbons and Mantle Helium in Oil and Gas Fields. In "The future of natural gas", D.G. Howell, ed., U.S. Geological Survey Professionnal Paper N°1570, pp. 31-56

Kharaka Y. K. and Specht D. J. (1988) The solubility of noble gases in crude oil at 25–100 1C. Appl. Geochem. 3: 137–144

Kennedy B.M., Hiyagon H. and Reynolds J.H. (1990) Crustal Neon: a striking uniformity. Earth Planet. Sci. Letters. 98: 277-286

Kennedy B.M., Torgersen T. and Van Soest M.C. (2002) Multiple atmospheric noble gas components in hydrocarbon reservoirs: A study of the Northwest Shelf, Delaware Basin, SE New Mexico. Geochim. Cosmochim. Acta. 66, N° 16: 2807-2822

Kipfer R., Aeschbach-Hertig W., Peeters F. and Stute M. (2002) Noble gas in lakes and ground waters. . In "Noble Gases in Geochemistry and Cosmoschemistry", Review in Mineralogy and Geochemistry. 47: 615-689

Kotarba M.J. and Nagao K. (2008) Composition and origin of natural gases accumulated in the Polish znd Ukrainian parts of the CArepathian region: Gaseous hydrocarbons, noble gases, carbon dioxide and nitrogen. Chemical Geol. 255: 426-438

Kurz M.D. and Jenkins W.J. (1981) The distribution of helium in oceanic basaltic glasses. Earth Planet Sci. Lett. 53: 41-54

Magnier C., Prinzhofer A., Flauraud E.and Giannesini S. (2011) Effective diffusion rates of CO_2 and associated noble gases in low permeability rocks. Submitted to OGST

Mamyrin B.A. and Tolstikhin, I. N. (1984) Helium isotopes in nature. Elsevier, Amsterdam, 273p.

Mazor E. and Bosh A. (1987) Noble gas in formations fluids from deep sedimentary basins: a review. Applied Geochemistry. 2: 621-627

Moreira M. and Allegre C.J. (1998) Helium-neon systematic and the structure of the mantle. Chem. Geol. 147: 53-59

Morrison P. and Pine J. (1955) Radiogenic origin of the helium isotopes in rocks. Ann. New York Acad. Sci. 62: 69-92

Nagao K., Takaoka N. and Matsubayashi O. (1981) Rare gas isotopic compositions in natural gases of Japan. Earth and Planet. Sci. Lett. 53: 175-188

O'Nions R.K. and Oxburg E.R. (1988) Helium, volatile fluxes and the development of the continental crust. Earth Planet. Sci. Lett. 90: 331-447

O'Nions R.K. and Ballentine C.J. (1993) Rare gas studies of basin scale fluid movement. Phil. Trans. R. Soc. London A. 344: 141-156

Oxburgh E.R., O'Nions R.K. and Hill R.I. (1986) Helium isotopes in sedimentary basins. Nature. 324, 18/24: 632-635

Palya, A. P., Buick, I. S., and Bebout, G. E. (2011) Storage and mobility of nitrogen in the continental crust: Evidence from partially melted metasedimentary rocks, Mt. Stafford, Australia. Chemical Geology. 281: 211-226

Pinti, D.L., and B. Marty (1995) Noble gases in crude oils from the Paris Basin, France: implications for the origin of fluids and constraints on oil-water-gas interactions. Geochim. Cosmochim. Acta. 59: 3389-3404

Podosek F.A., Bernatowicz T.J. and Kramer F.E.(1982) Adsorption of xenon and krypton on shales. Geochim. Cosmochim. Acta. 45, N° 12: 2401-2415

Porcelli D., Ballentine C.J. and Wieler R. (2002) An overview of Noble Gas geochemistry and cosmochemistry. In "Noble Gases in Geochemistry and Cosmoschemistry", Review in Mineralogy and Geochemistry. 47: 1-20

Prinzhofer A. and Pernaton E. (1997) Isotopically light methane in natural gases: bacterial imprint or segregative migration? Chemical Geology. 142: 193-200

Prinzhofer A., Guzman-Vega M. A., Battani A & Escudero M. (2000) Gas geochemistry of the Macuspana Basin, Mexico : thermogenic accumulations in sediments impregnated by bacterial gas. Marine and Petroleum Geology. 17: 1029-1040

Prinzhofer A. & Battani A. (2003) Gas isotope tracing: an important tool for hydrocarbon exploration. Revue de l'IFP, Special Publication for B. Tissot's Jubilee, June 2003. Oil and Gas Science and Technology. Rev. IFP. 58, N° 2: 299-311

Prinzhofer A., Vaz Dos Santos Neto E. and Battani A. (2010) Coupled use of carbon isotopes and noble gas isotopes in the Potiguar basin (Brazil): Fluids migration and mantle influence. Marine and Petroleum Geology. 27: 1273-1284

Rebour V, Billotte J., Deveugele M, Jambon A. and le Guen C. (1997) Molecular diffusion in water saturated rocks : A new experimental method. J. Cont. Hydrol. 28: 71-93

Reid R.C., Praunsnitz J.M. and Sherwood T.K. (1977) The properties of gases and liquids. McGraw-Hill Ed., 688p

Ricard E., Pecheyran C., Ortega G.S., Prinzhofer A. and Donard O.F. X. (2011) Direct analysis of trace elements in crude oils by high-repetition-rate femtosecond laser ablation coupled to ICPMS detection. Anal Bioanal Chem. 399 2153–2165

Rudnick R. and Fountain D.M. (1995) Nature and composition of the continental crust: A lower crustal perspective. Rev. Geophys. 33: 267-309

Sano Y., Tominaga T. and Wakita H. (1982) Elemental and isotopic abundance of rare gases in natural gases obtained by a quadrupole mass spectrometer. Geochem. J. 16: 279-286

Sano Y., Watika H. and Huang C.W. (1986) Helium flux in a continental land area from 3He/4He ratio in northern Taiwan. Nature. 323: 55-57

Sarda P., Staudacher T. and Allegre C.J. (1988) Neon isotopes in submarine basalts. Earth Planet. Sci. Lett. 91: 73-88

Sherwood-Lollar B., Weise S.M., Frape S.K. and Barker J.F. (1994) Isotopic constraints on the migration of hydrocarbon and helium gases of southwestern Ontario. Bull. Of Canadian Petroleum Geology. 42, N° 3: 283-295

Sherwood-Lollar B., Ballentine C.J. and O´Nions R.K. (1997) The fate of mantle-derived carbon in a continental sedimentary basin: Integration of CHe relationships and stable isotope signatures. Geochim. Cosmochim. Acta. 61, Issue 11: 2295-2307

Smith S.P. and Kennedy B.M. (1983) The solubility of noble gas in water and in NaCl brine. Geochim. Cosmochim. Acta. 47: 503-515

Smith S.P. (1985) Noble gas solubility at high temperature. EOS, Trans. Am. Geophys. Union. 66: 397

Staudacher T., Sarda P., Richardson S.H., Allegre C.J., Sagna I and Dmitriev L.V. (1989) Noble gas in basalt glasses from a Mid-Atlantic Ridge topographic high at 14°N. Geodynamic consequences. Earth Planet. Sci. Lett. 96: 119-133

Steiger R.H. and Jager E. (1977) Subcommission on geochronology: convention on the use of decay constants in geo- and cosmochronology. Earth Planet. Sci. Lett. 36: 359-362

Stuart F.M, Lass-Evans S., Fitton G. and Ellam R.M. (2003) High 3He/4He ratios in picritic basalts from Baffin Island and the role of a mixed reservoir in mantle plumes. Nature. 424(6944): 57-9

Torgersen T. and Kennedy B.M. (1999) Ar-Xe enrichments in Elk Hills oil field gases: role of water in migration and storage. Earth Planet. Sci. Letter. 167: 239-253

Trieloff M., Kunz J., Clague D.A., Harrison D. and Allegre C.J. (2000) The nature of pristine noble gases in mantle plumes. Science. 288: 1036-1039

Trieloff M., Kunz J. and Allegre C.J. (2002) Noble gas systematic of the Réunion mantle plume source and the origin of primordial noble gases in Earth´s mantle. Earth Planet. Sci. Letters. 200: 297-313

Vacquand C., Guyot F., Prinzhofer A. and Magnier C. (2011) An experimental study of hydrogen migration through water saturated porous rocks. Submitted to OGST.

Wacker1985 J.F., Zadnik M.G. and Anders E. (1985) Laboratory simulation of meteoritic noble gases. I. Sorption of xenon on carbon: trapping experiments. Geochim. Cosmochim. Acta. 49: 1035-1048

Wacker J.F. (1989) Laboratory simulation of meteoritic noble gases. III. Sorption of neon, argon, krypton and xenon on carbon. Elemental fractionation. Geochim. Cosmochim. Acta. 53: 1421-1433

Wasserburg G.J., Mazor E. and Zartman R.E. (1963) Isotopic and chemical composition of some terrestriam natural gases. In: Earth Science and Meteorites, Geiss and Goldberg Editors p. 219-240

Weis R.F. (1970) The solubility of nitrogen, oxygen and argon in water band seawater Deep-Sea Research. 17: 721-735

Weis R.F. (1971) Solubility of helium and neon in water and seawater. J. Chem. Eng. Data. 16: 235-241

Weis R.F. and Kyser T.K. (1978) Solubility of krypton in water and seawater. J. Chem. Eng. Data. 23: 69-72

Xu S., Nakai S. Wakita H. and Wang X (1995) Mantle-derived noble gases in natural gases from Songliao Basin, China. Geochem. Cosmochem. Acta. 59: 4675-4683

Yang J, Lewis R.S. and Anders E. (1982) Sorption of noble gases by solids, with reference to meteorites. I. Magnetite and carbon. Geochim. Cosmochim. Acta. 46: 841-860

Yu S., Lu X., Xu H., Xie Q. and Liu X. (2010) Geochemical evidence for differential accumulation of natural gas in Shiwu fault depression, Songliao Basin, China. Energy Exploration & Exploitation. 28, N° 4: 239-258

Zartman R.E. and Wasserburg G.J. (1961) Helium, Argon, and Carbon in Some Natural Gases. Journal of Geophysical Research. 66, N° 1: 277-306

Zhou Z., Ballentine C.J., Kipfer R., Schoell M. and Thibodeaux S. (2005) Noble gas tracing of groundwater/coalbed methane interaction in the San Juan Basin, USA. Geochimica et Cosmochimica Acta. 69, Issue 23: 5413-5428

Zhou Z. And Ballentine C.J. (2006) ^{4}He dating of groundwater associated with hydrocarbon reservoirs Chemical Geology. 226, Issues 3–4: 309-327

Table captions

Table 1: Average concentrations and isotopic ratios of the principal reservoirs of noble gas compounds affecting a petroleum system. The atmospheric concentration values are in ppm mol/mol (Porcelli et al., 2002). The ASW concentration values are in micromoles per cubic meter (Kipfer at al., 2002). The MORB concentration values are normalized to the ^{36}Ar concentrations (Burnard et al., 1997; Moreira M. and Allegre C.J., 1998). Only the isotopic ratios of the continental crust have been represented, as the range of variation of noble gas concentrations may be very large.

Table 2: Values of the solubility coefficients in $(mol/m^3)/(mol/m^3)$, between gas and water, heavy oil (API 25) and gas, and light (API 34) and gas, for atmospheric pressure and temperatures between 10 and 170°C. Values calculated from Smith and Kennedy, (1983), Smith (1985), Harvey (1998) and Kharaka and Specht (1988).

Figure captions

Figure 1: Shematic diagram of a petroleum system with the different possible origins of noble gases entering into a hydrocarbon accumulation (from Ballentine and O'Nions, 1994, modified).

Figure 2: Relative noble gas solubilities between light oil and water as a function of temperature at atmospheric pressure (from Kharaka and Specht 1988).

Figure 3: Partition coefficients of noble gases between oil, water and gas phases, in $(mol/m^3)/mol/m^3)$ at atmospheric pressure and 50°C.

Figure 4: Concentrations of noble gases in three oil, water and gas, that had originally equilibrated with ASW (Air Saturated Water), and with volume ratios gas/water and oil/water of 0.1 m^3/m^3. All the concentrations are normalized to ASW values.

Figure 5: Evolution of $^{84}Kr/^{20}Ne$ and $^{36}Ar/^{20}Ne$ ratios for oil, water and gas phases at thermodynamic equilibrium, for temperatures varying from 0 to 230°C, and gas/water and oil/water ratios of 0.01 m^3/m^3. Dots represent temperature steps of 10°C between 0 and 30°C, and steps of 20°C between 30 and 230°C.

Figure 6: Air-normalized concentrations of noble gas compounds for kerogen and shale samples (Frick and Chang, 1977), expressed in mol/m^3. The concentrations of ASW are also represented.

Figure 7: Correlation between the solubility coefficient of different gases in water (in $(mol/m^3)/(mol/m^3)$ at room temperature and atmospheric pressure) and the diffusion coefficients in water (in m^2/s). Data from Crovetto et al. (1981), Smith and Kennedy (1983), Smith (1985), Harvey (1998) for the solubilities, and Jähne et al. (1987) and Reid et al. (1977) for the diffusion coefficients.

Figure 8: Product of the solubility and diffusion coefficients in water for the series of noble gas compounds, showing the non-monotonous trend of this key parameter for diffusive fluxes in porous rocks. Same references as Figure 7.

Figure 9: Correlation of the Gas/Water ratios (in m^3/m^3) calculated with the concentrations of ^{36}Ar and ^{84}Kr in different gas accumulations worldwide. Data from Ballentine et al., 1991, 1996; Ballentine and Sherwood-Lollar, 2002; Prinzhofer and Battani, 2003; Gilfillan et al., 2009; Prinzhofer et al., 2010; Battani et al., 2011.

Figure 10: Calculation of the Gas/Water ratios calculated with three ASW noble gases, ^{20}Ne, ^{36}Ar and ^{84}Kr. a: gas samples accumulated in a Brazilian Cenozoic Basin. b: gas samples accumulated in a Brazilian Paleozoic Basin. Prinzhofer and Battani, 2003; Prinzhofer et al., 2010.

Figure 11: Gas/Water ratios calculated with ASW noble gases, ^{20}Ne, ^{36}Ar and ^{84}Kr for the oil associated gas samples collected at well heads of oil fields in the Trinidad Islands (in red) and for gas sampled at the head of mud volcanoes from the same area in the Trinidad Islands. Data from Battani et al., 2011.

Figure 12: Correlation between the carbon isotopic ratios of methane and Gas/Water ratios calculated with ^{84}Kr, for gas samples associated with biodegraded oils of the Potiguar Basin, Brazil (data from Prinzhofer et al., 2010).

Figure 13: Two gas families from the Makran (Pakistan) mud volcanoes (Ellouz-Zimmermann et al., 2007). The green squares correspond to bacterial gas generation, whereas the red circles correspond to thermogenic gases seeping through the mud volcano vents. a: carbon isotopic signatures of CO_2 and CH_4. b: $^4He/^{40}Ar^*$ ratios versus the reciprocal of ^{136}Xe concentrations.

Figure 14: The age (in million years) calculated for gases from the Pakistan mud volcanoes (see Figure 13). A correlation exists between the "ages" calculated using ^4He-^{36}Ar and those using ^{40}Ar-^{36}Ar.

Figure 15: Correlation between the radiogenic isotope $^{40}Ar^*$ and the fossil ^{36}Ar for two series of oil and gas accumulations in a Paleozoic Basin (Prinzhofer and Battani, 2003). The two trends with two different slopes correspond to oil fields with different resident times.

Figure 16: Schematic sketch representing the relation between the efficiency of accumulation of a hydrocarbon field, its average maturity and its average residence time: For the same maturity history of a source rock; a field with a poor efficiency of accumulation will produce a fluid with higher maturity and lower residence time (and possibly higher nitrogen concentrations).

Figure 17: For oil and gas accumulations in a Paleozoic Basin (Prinzhofer and Battani, 2003), diagrams interpreting the possible mantle influence in the hydrocarbon accumulations. a: Ratios $CO_2/^3He$ versus $^3He/^4He$ normalized to the atmospheric ratio as R/Ra. b: Correlation between the argon isotopic ratio $^{40}Ar/^{36}Ar$ and the helium isotopic ratio $^3He/^4He$ expressed as R/Ra. c: Correlation between the concentrations of ^3He and ^4He.

Figure 18: Relation between the carbon isotopic ratio of carbon dioxide and its concentration in gas accumulations, for different basins wordwide (Ballentine et al., 1991, 1996; Prinzhofer et al., 2000; Ballentine and Sherwood-Lollar, 2002; Deville et al., 2003; Prinzhofer and

Battani, 2003; Ellouz-Zimmermann et al., 2007; Gilfillan et al., 2009; Prinzhofer et al., 2010; Battani et al., 2011).

Figure 19: Helium isotopic ratios of gas accumulations, expressed as R/Ra, versus the carbon dioxide concentrations in the gas accumulations. Same database as Figure 18.

Figure 20: Correlation between the argon isotopic ratio $^{40}Ar/^{36}Ar$ and the helium isotopic ratio $^{3}He/^{4}He$ expressed as R/Ra for the same database as Figure 18.

Figure 21: Mixing diagram using $^{20}Ne/^{4}He$ versus the helium isotopic ratio expressed as R/Ra. The database is the same as for Figure 18.

Figure 22: $^{20}Ne/^{22}Ne$ versus $^{21}Ne/^{22}Ne$ for CO_2-rich gas accumulations studied by Gilfillan et al., (2009).

Figure 23: $^{84}Kr/^{20}Ne$ versus $^{36}Ar/^{20}Ne$ for a large wordwide gas database. The end-members of the atmosphere and of ASW are also shown.

Figure 24: Same diagram as Figure 24 for the CO_2-rich gas accumulations studied by Gilfillan et al., (2009).

Figure 25: Correlation between the helium and nitrogen concentrations of the Hugoton, Panhandle and Bush Dome gas accumulations (from Brown, 2010).

	^{4}He	^{20}Ne	^{36}Ar	^{84}Kr	^{132}Xe	R/Ra	^{20}Ne/^{22}Ne	^{21}Ne/^{22}Ne	^{40}Ar/^{36}Ar
Atmosphere (ppm)	5.24	16.5	31.4	0.65	0.023	1	9.8	0.029	295.5
ASW (20°C, fresh water) μmol/m3	2.04	7.67	47.8	1.83	0.039	1	9.8	0.029	295.5
MORB Mantle	36,600	1.04	1	0.029	0.004	8	12.5 - 13.8	0.06 - 0.063	40,000
Continental crust	-	-	-	-	-	0.02	0.08 – 0,10	0.4 – 0.52	3,000

Atmosphere: Porcelli et al., 2002
Mantle: Moreira and Allegre, 1998, concentrations normalized to ^{36}Ar
Continental crust: Ballentine and Burnard, 2002

Table 1

solubility water/gas (mol/m^3)/(mol/m^3) 1 bar

T (°C)	He	Ne	Ar	Kr	Xe
10	0,0089	0,0111	0,0407	0,0795	0,1515
50	0,0090	0,0096	0,0236	0,0388	0,0603
110	0,0125	0,0111	0,0199	0,0281	0,0394
170	0,0209	0,0163	0,0253	0,0326	0,0465

Solubility heavy oil/gas (mol/m^3)/(mol/m^3) 1 bar

T (°C)	He	Ne	Ar	Kr	Xe
10	0,0128	0,0111	0,154	0,477	1,491
50	0,0211	0,0198	0,158	0,400	1,080
110	0,0445	0,0474	0,165	0,308	0,666
170	0,0939	0,1131	0,172	0,237	0,411

Solubility light oil/gas (mol/m^3)/(mol/m^3) 1 bar

T (°C)	He	Ne	Ar	Kr	Xe
10	0,0192	0,0236	0,163	0,504	2,256
50	0,0269	0,0317	0,149	0,443	1,397
110	0,0449	0,0494	0,130	0,365	0,681
170	0,0749	0,0768	0,113	0,301	0,332

Table 2

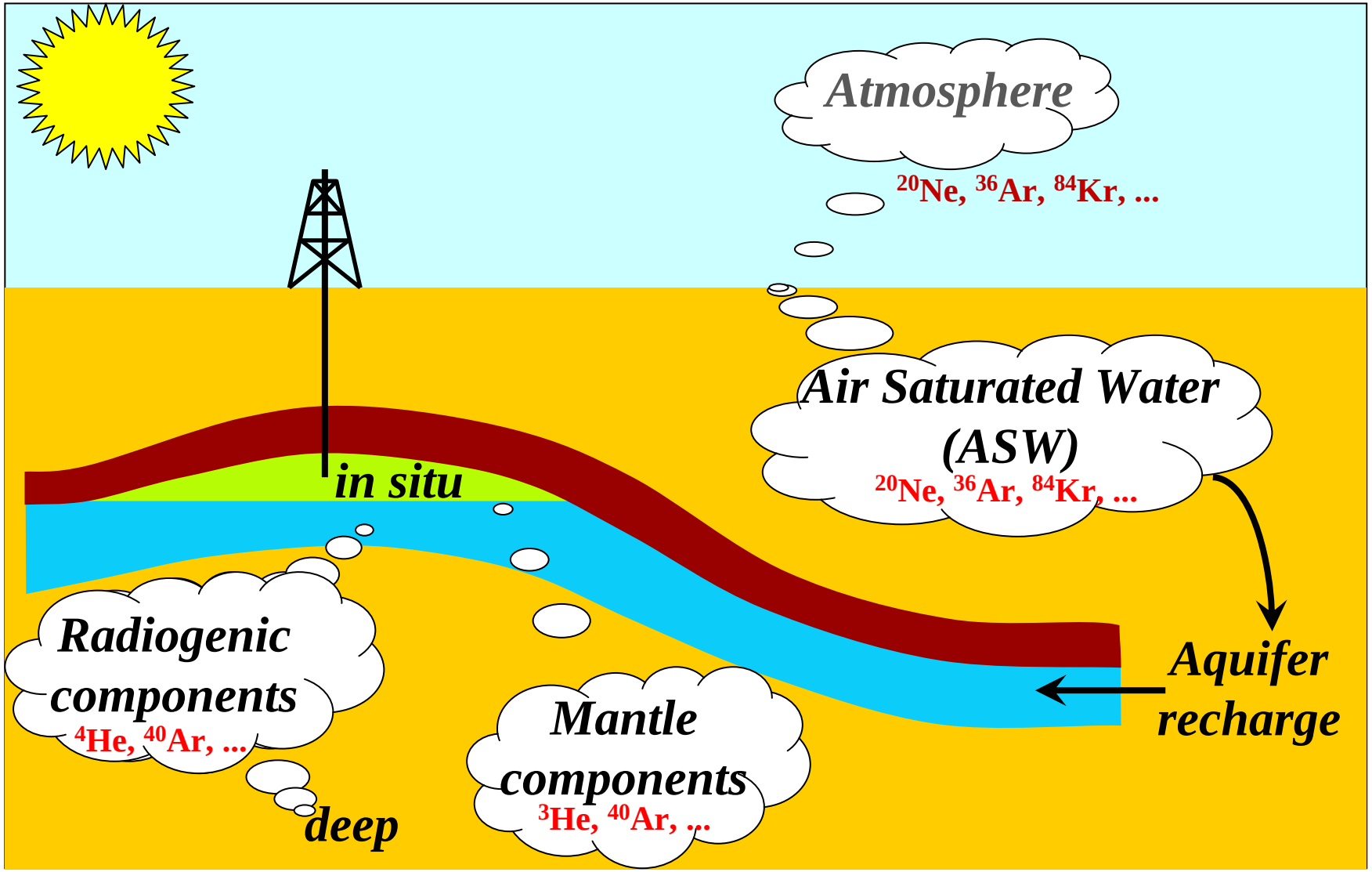
Atmosphere
^{20}Ne, ^{36}Ar, ^{84}Kr, ...
Air Saturated Water
(ASW)
^{20}Ne, ^{36}Ar, ^{84}Kr, ...
in situ
Radiogenic
components
^{4}He, ^{40}Ar, ...
deep
Mantle
components
^{3}He, ^{40}Ar, ..
Aquifer
recharge

Figure 1

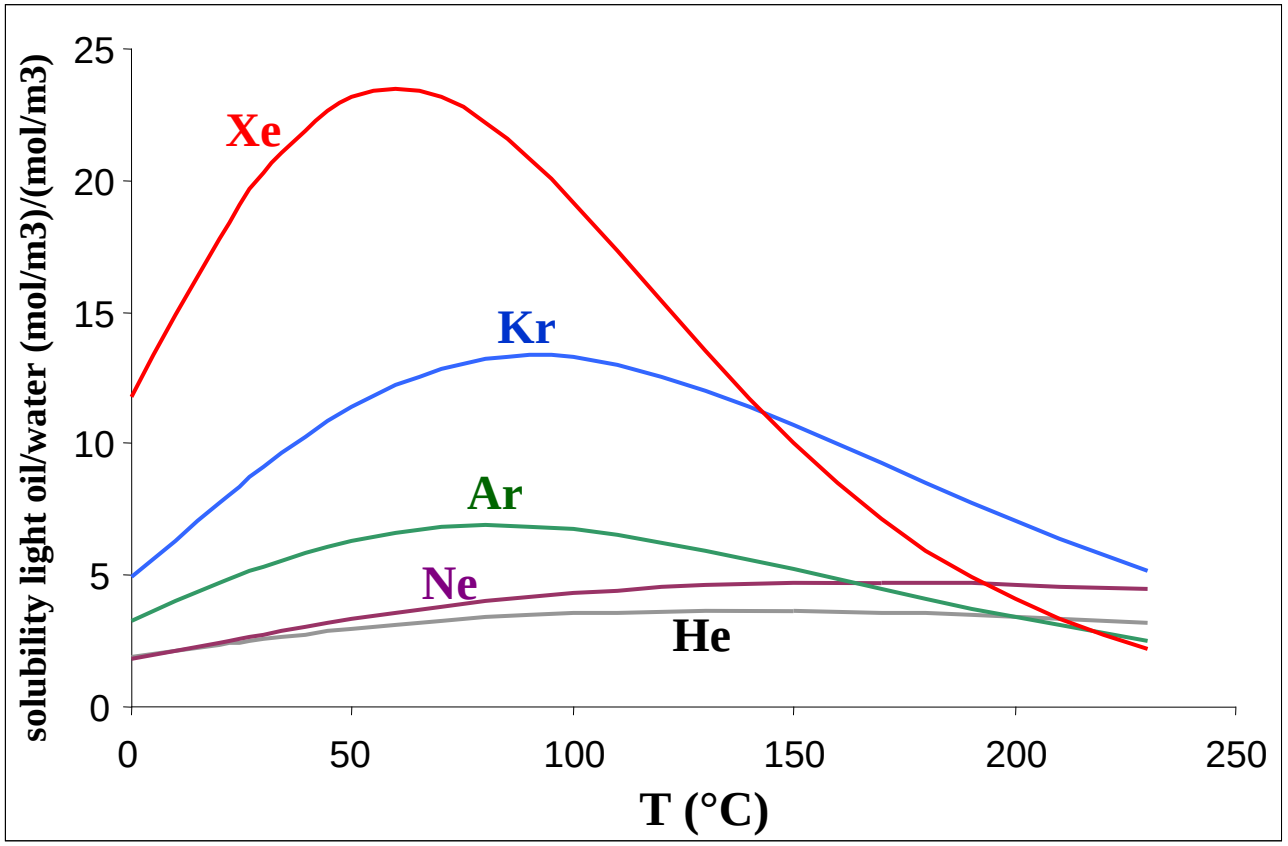
solubility light oil/water (mol/m3)/(mol/m3)
25
20
15
10
5
0
0
50
100
150
200
250
T (°C)
Xe
Kr
Ar
Ne
He

Figure 2

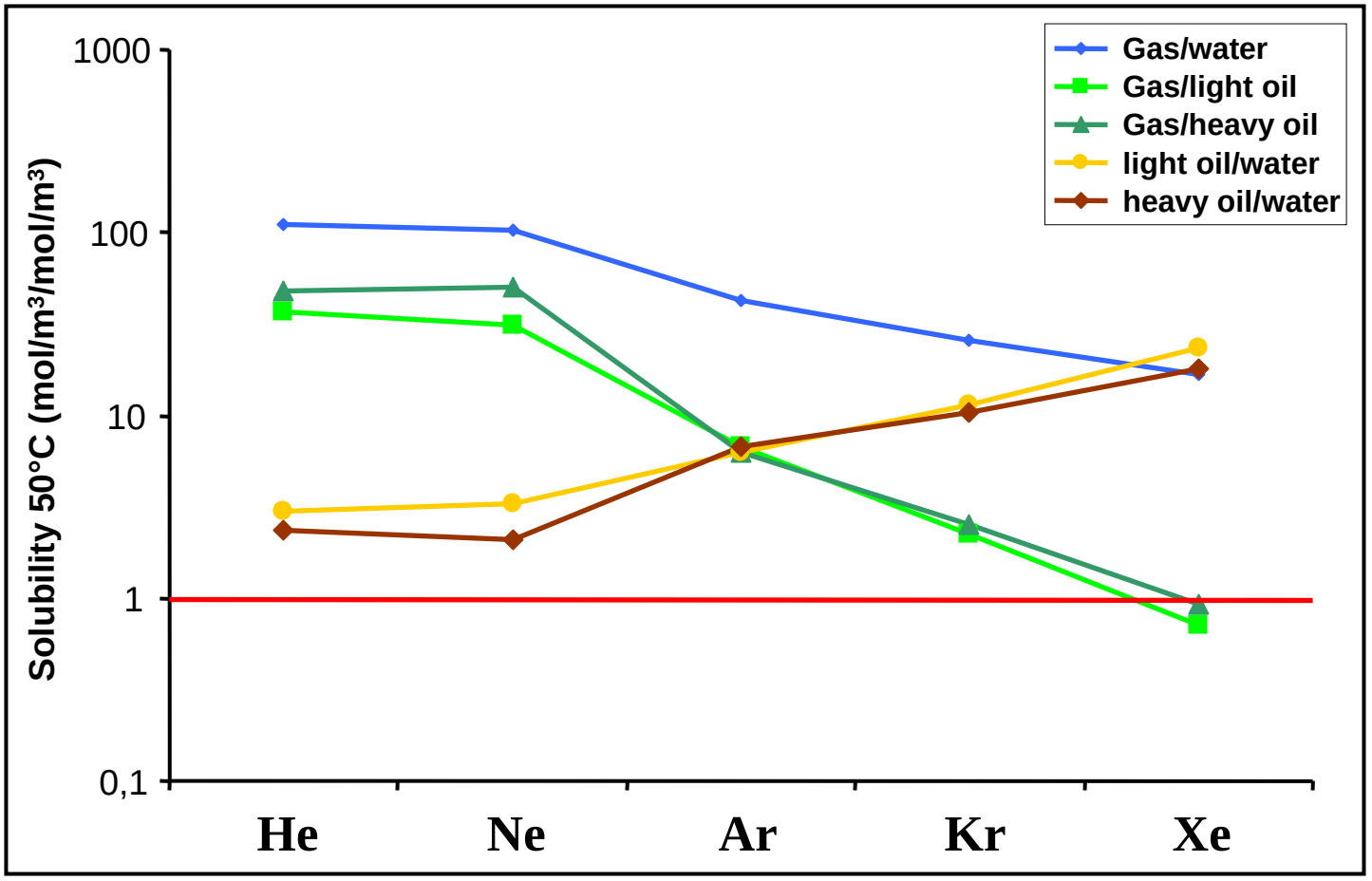
Gas/water
Gas/light oil
Gas/heavy oil
light oil/water
heavy oil/water
Solubility 50°C (mol/m³/mol/m³)
1000
100
10
1
0,1
He
Ne
Ar
Kr
Xe

Figure 3

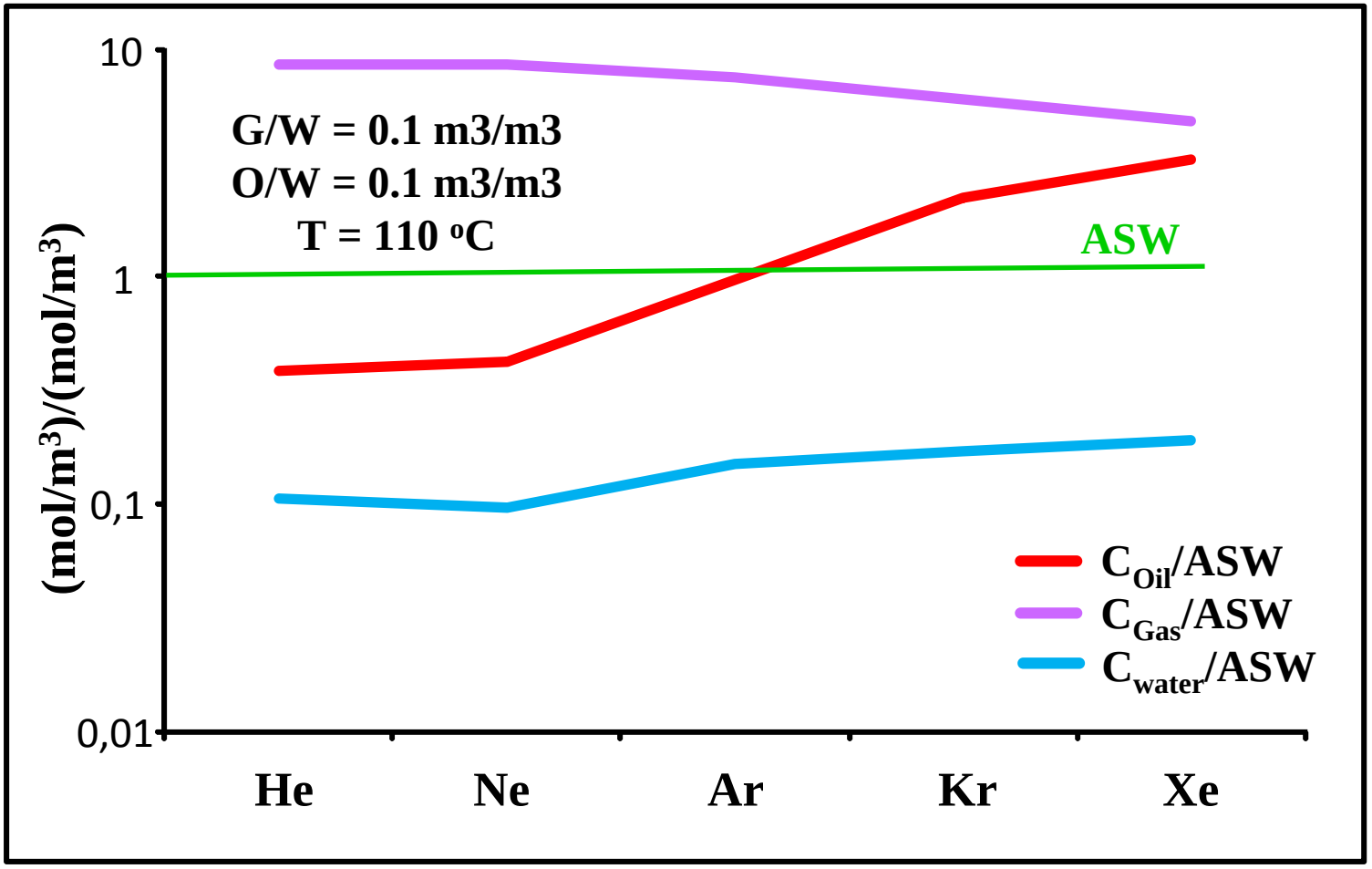
10
1
0,1
0,01
(mol/m3)/(mol/m3)
G/W = 0.1 m3/m3
O/W = 0.1 m3/m3
T = 110 oC
ASW
COil/ASW
CGas/ASW
Cwater/ASW
He
Ne
Ar
Kr
Xe

Figure 4

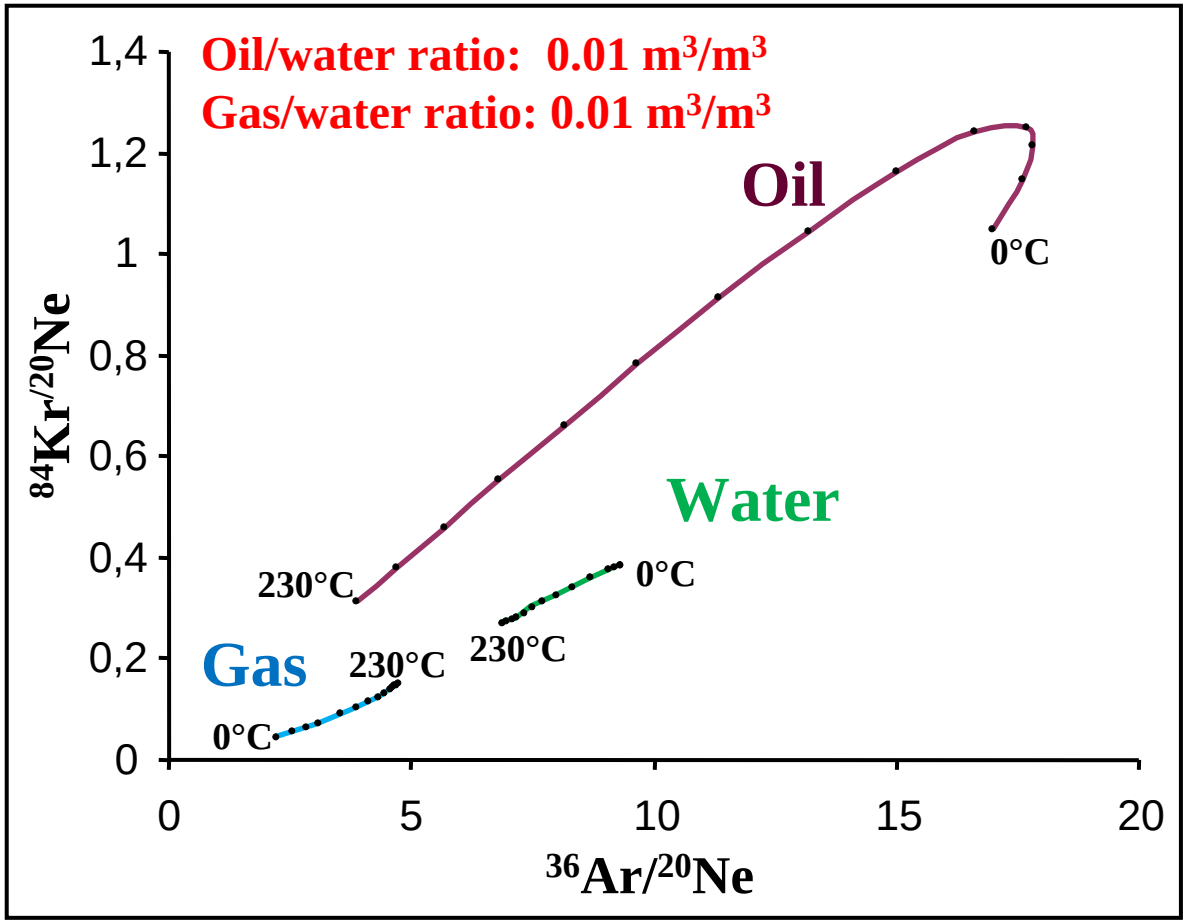
Oil/water ratio: 0.01 m3/m3
Gas/water ratio: 0.01 m3/m3
Oil
Water
Gas
0°C
230°C
230°C
0°C
230°C
0°C
84Kr/20Ne
36Ar/20Ne
1,4
1,2
1
0,8
0,6
0,4
0,2
0
0
5
10
15
20

Figure 5

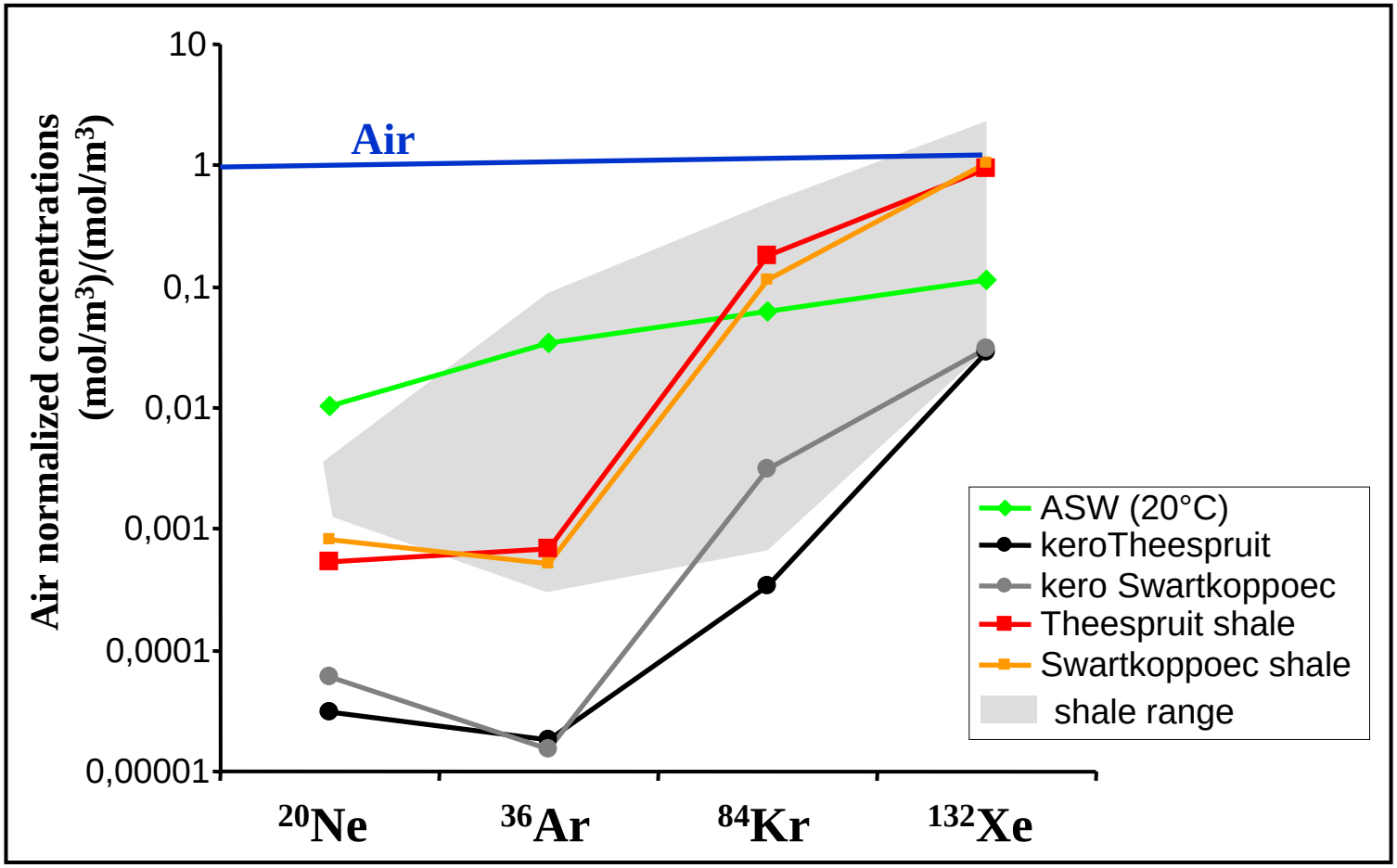
Air normalized concentrations (mol/m3)/(mol/m3)
10
1
0,1
0,01
0,001
0,0001
0,00001
Air
20Ne
36Ar
84Kr
132Xe
ASW (20°C)
keroTheespruit
kero Swartkoppoec
Theespruit shale
Swartkoppoec shale
shale range

Figure 6

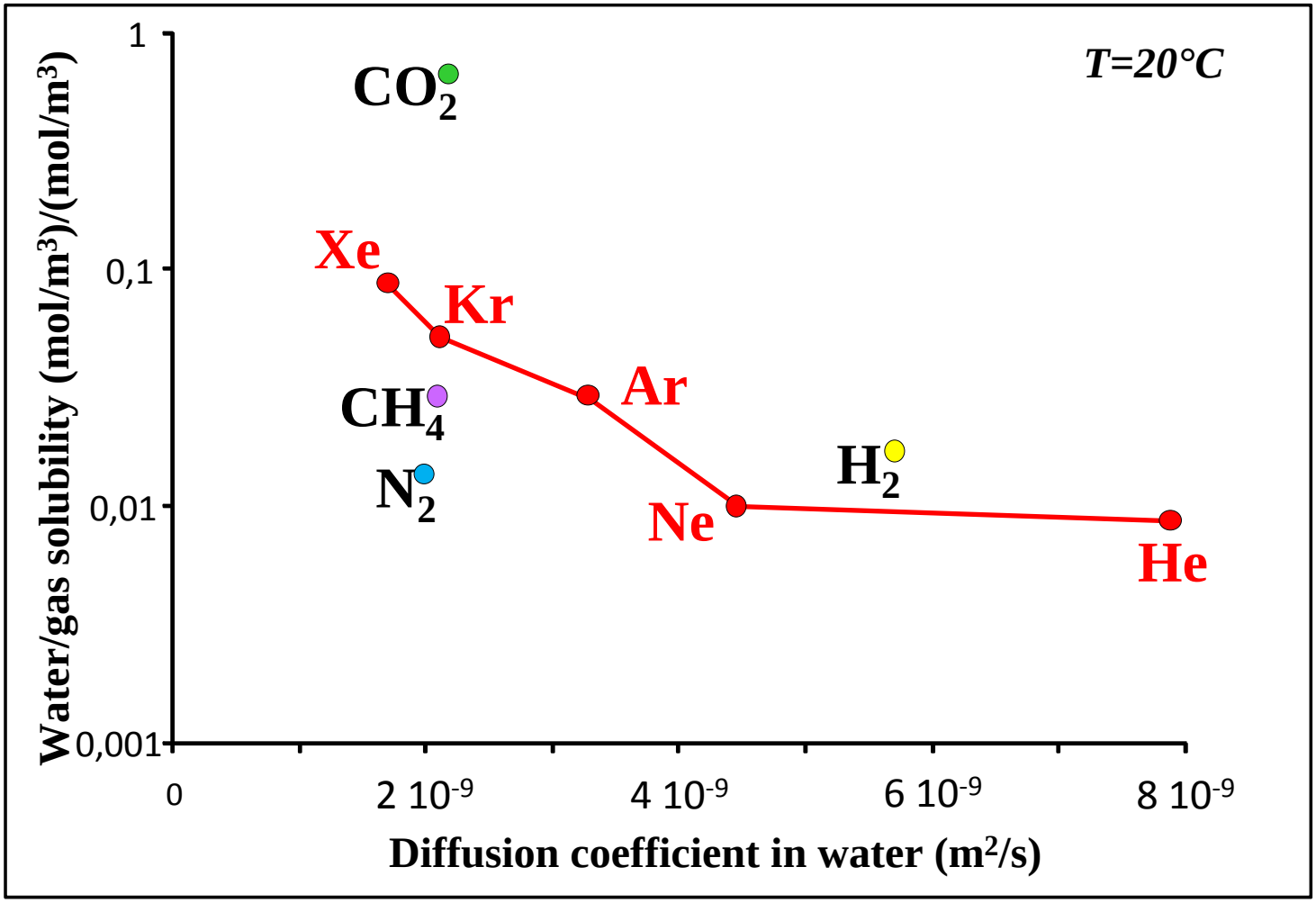
T=20°C
CO2
Xe
Kr
Ar
CH4
N2
H2
Ne
He
1
0,1
0,01
0,001
0
2 10-9
4 10-9
6 10-9
8 10-9
Water/gas solubility (mol/m3)/(mol/m3)
Diffusion coefficient in water (m2/s)

Figure 7

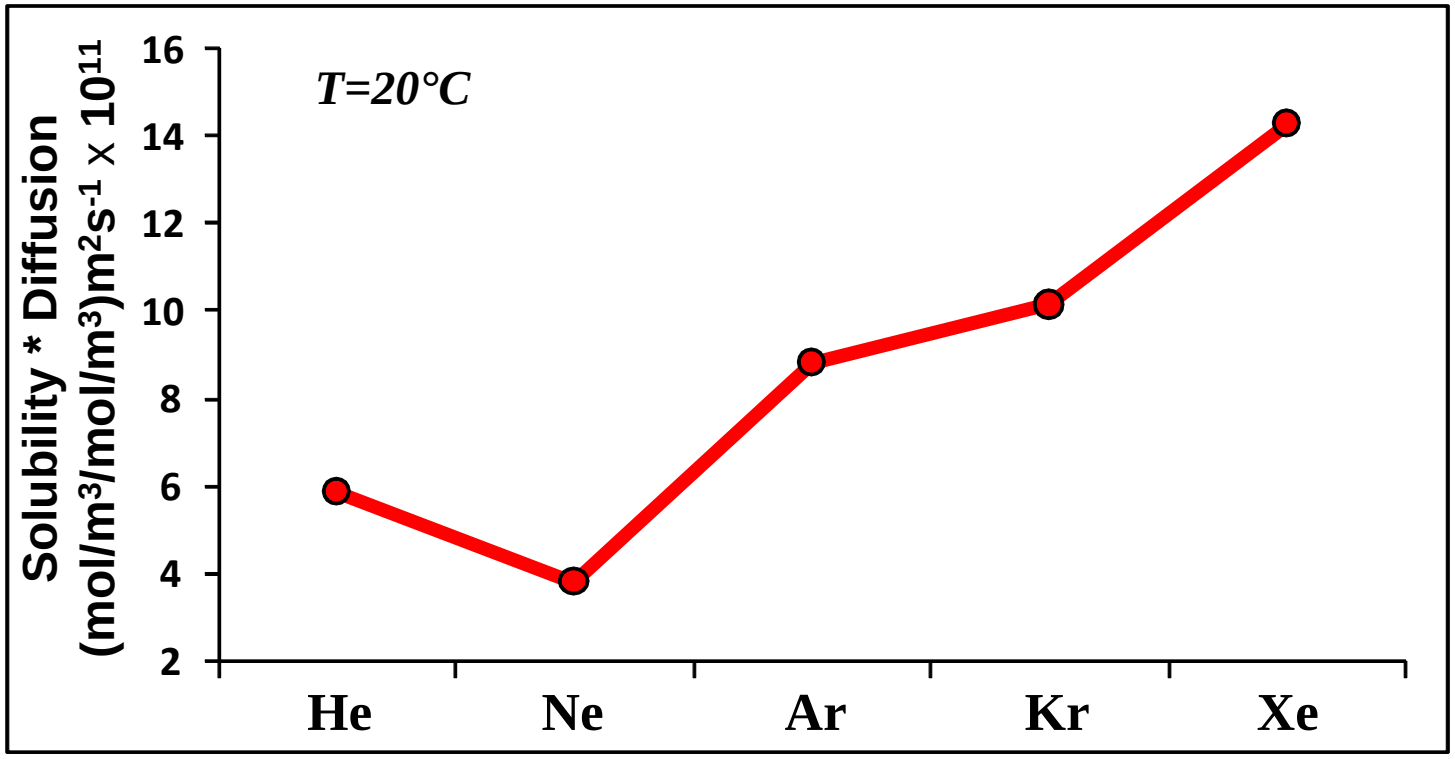
Solubility * Diffusion
(mol/m³/mol/m³)m²s⁻¹ X 10¹¹
16
14
12
10
8
6
4
2
T=20°C
He
Ne
Ar
Kr
Xe

Figure 8

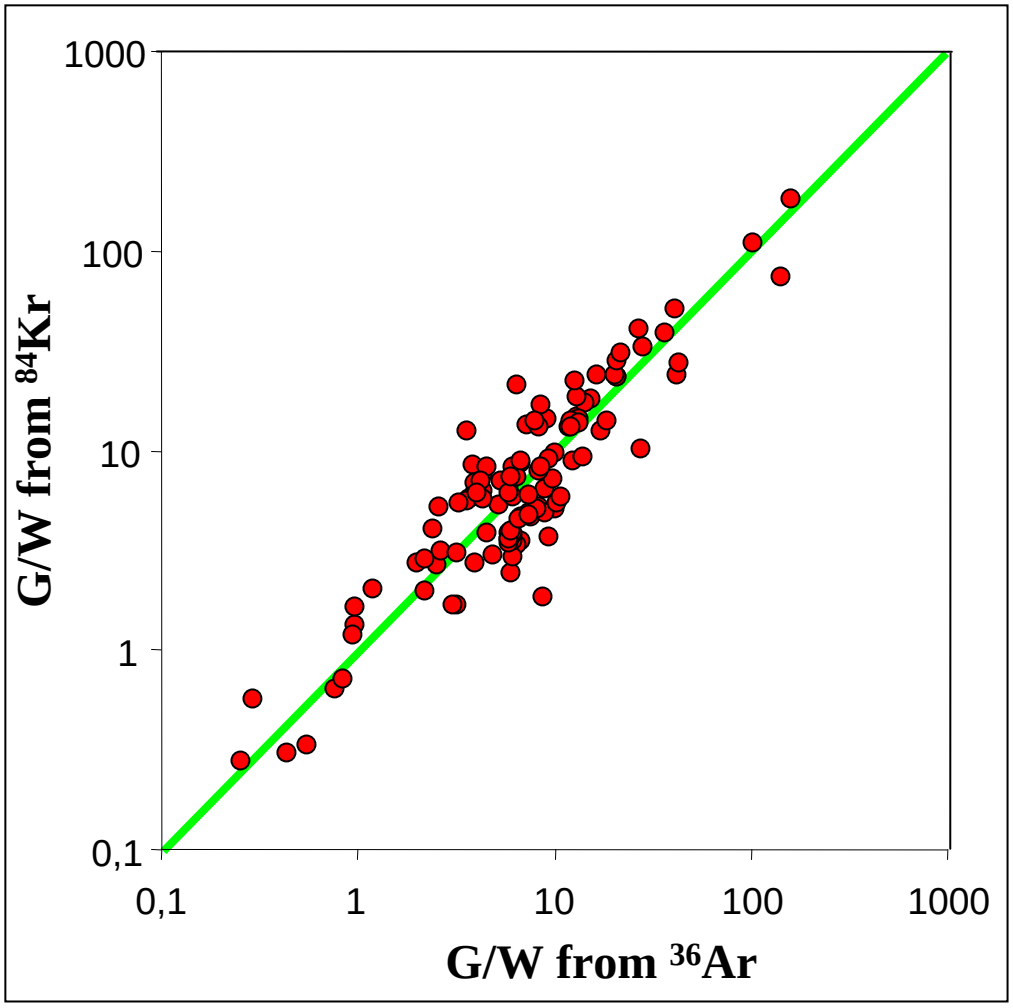

Figure 9

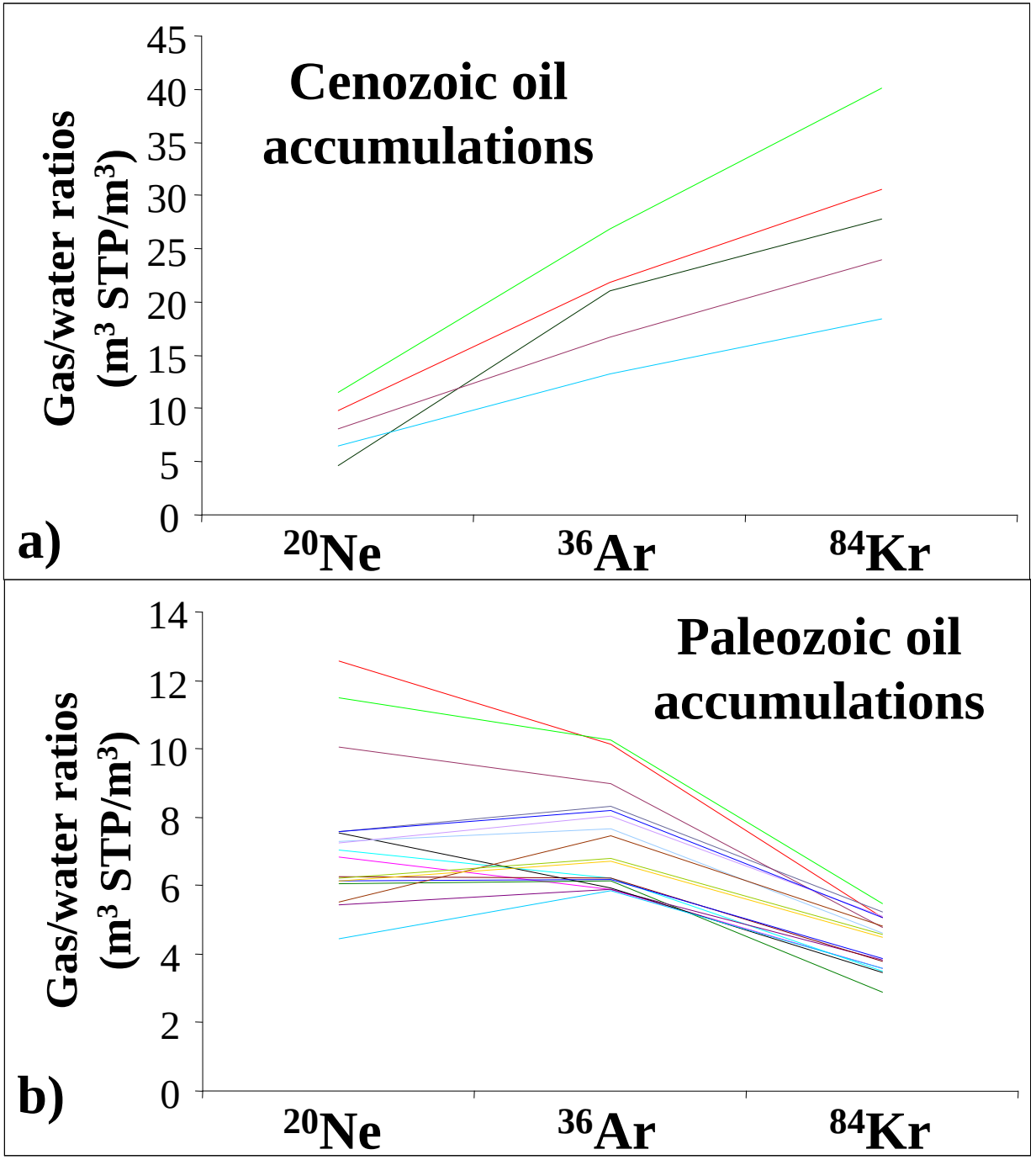
Cenozoic oil accumulations
Gas/water ratios (m3 STP/m3)
45
40
35
30
25
20
15
10
5
0
a)
20Ne
36Ar
84Kr
Paleozoic oil accumulations
Gas/water ratios (m3 STP/m3)
14
12
10
8
6
4
2
0
b)
20Ne
36Ar
84Kr

Figure 10

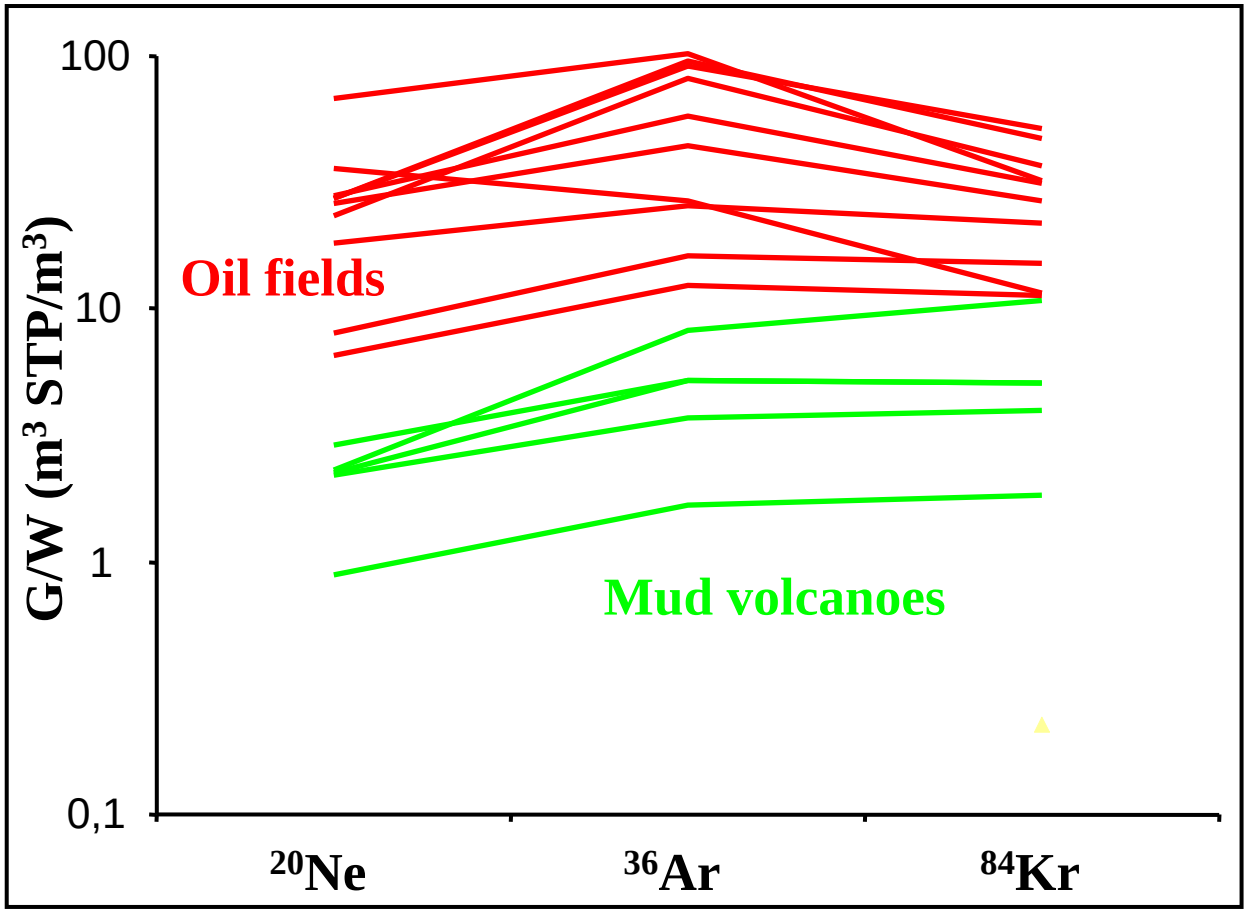
100
10
1
0,1
G/W (m3 STP/m3)
Oil fields
Mud volcanoes
20Ne
36Ar
84Kr

Figure 11

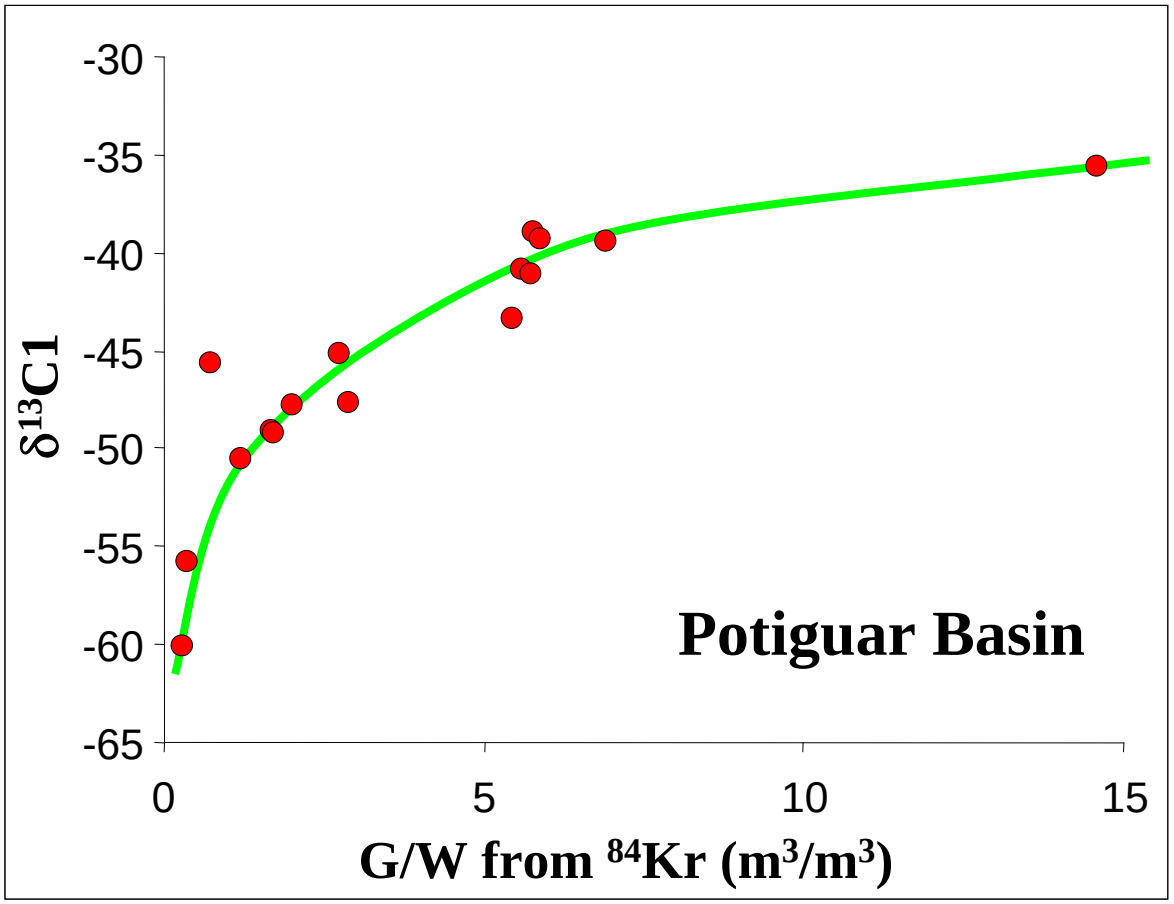
-30
-35
-40
-45
-50
-55
-60
-65
δ13C1
0
5
10
15
G/W from 84Kr (m3/m3)
Potiguar Basin

Figure 12

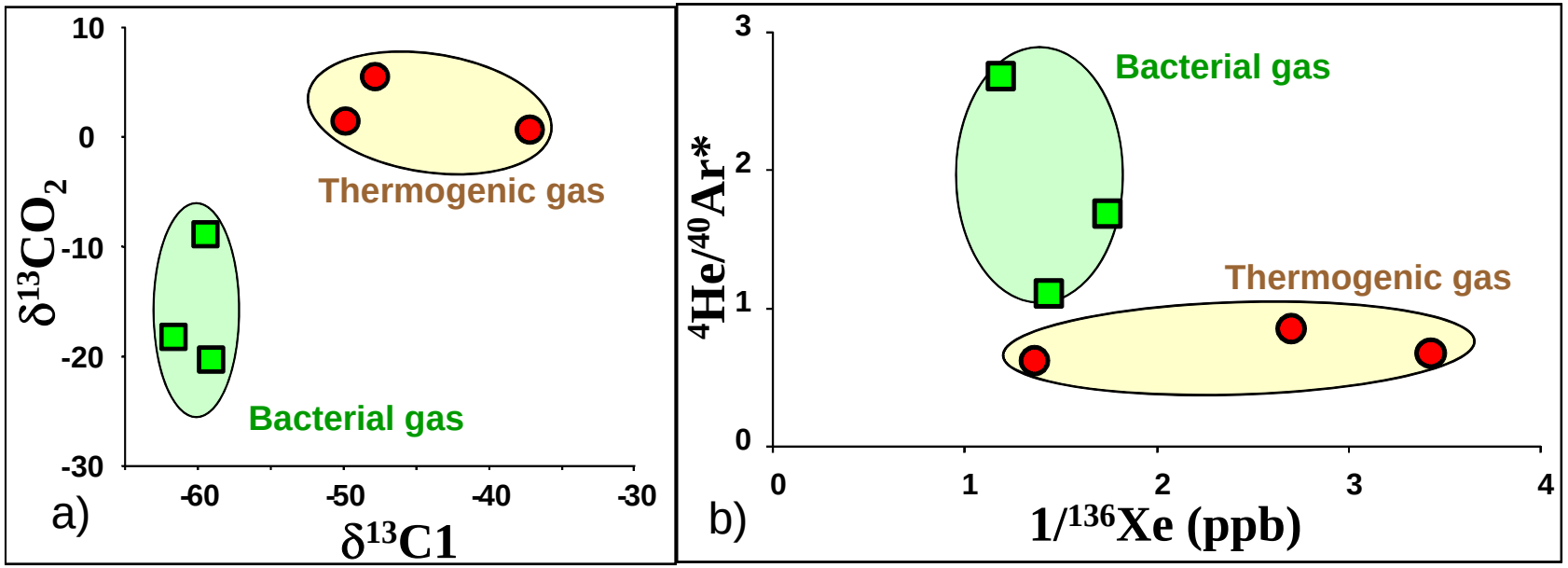
10
0
-10
-20
-30
$\delta^{13}CO_2$
-60
-50
-40
-30
$\delta^{13}C1$
a)
Thermogenic gas
Bacterial gas
3
2
1
0
$^4He/^{40}Ar^*$
0
1
2
3
4
$1/^{136}Xe$ (ppb)
b)
Bacterial gas
Thermogenic gas

Figure 13

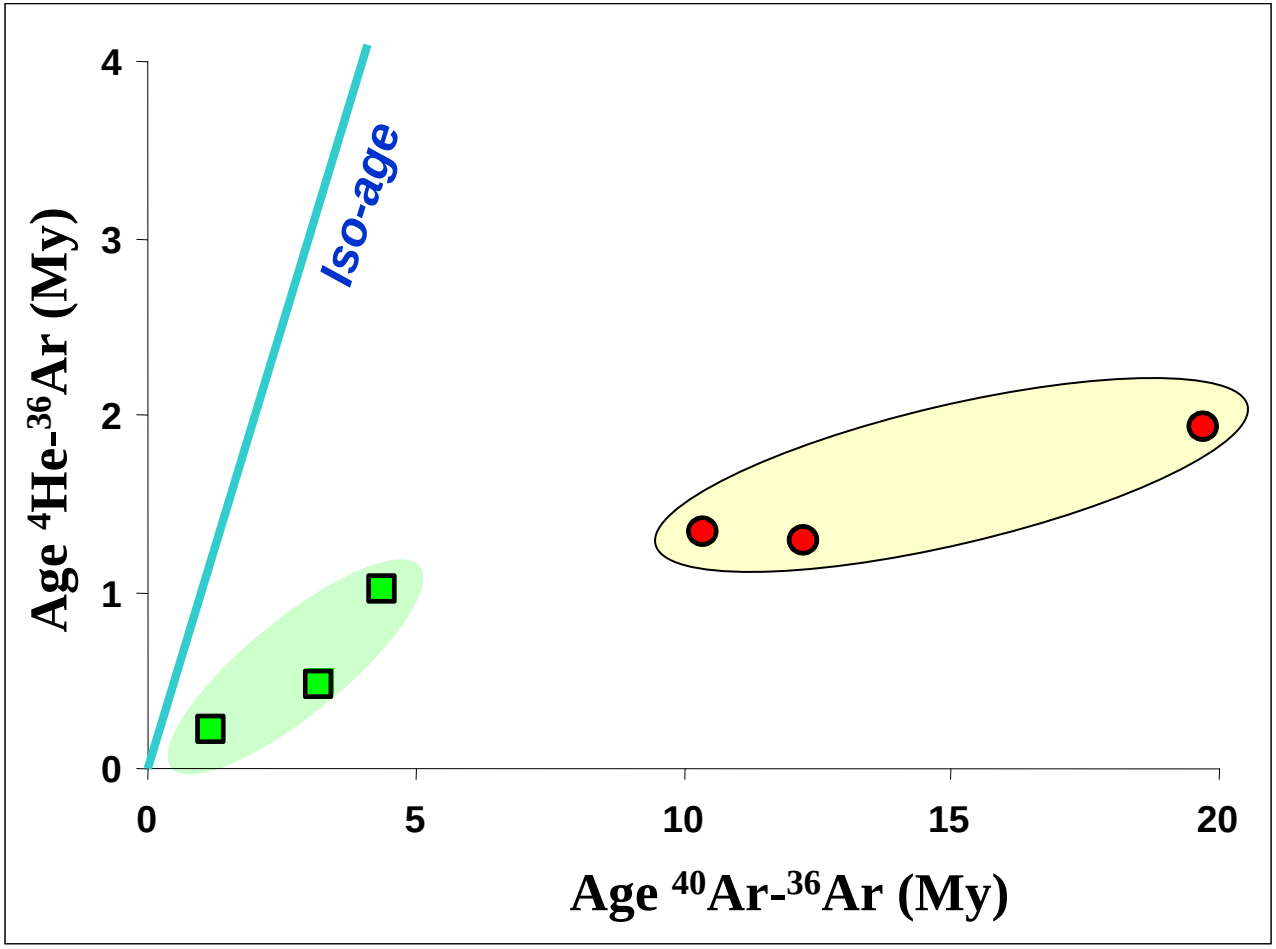

Figure 14

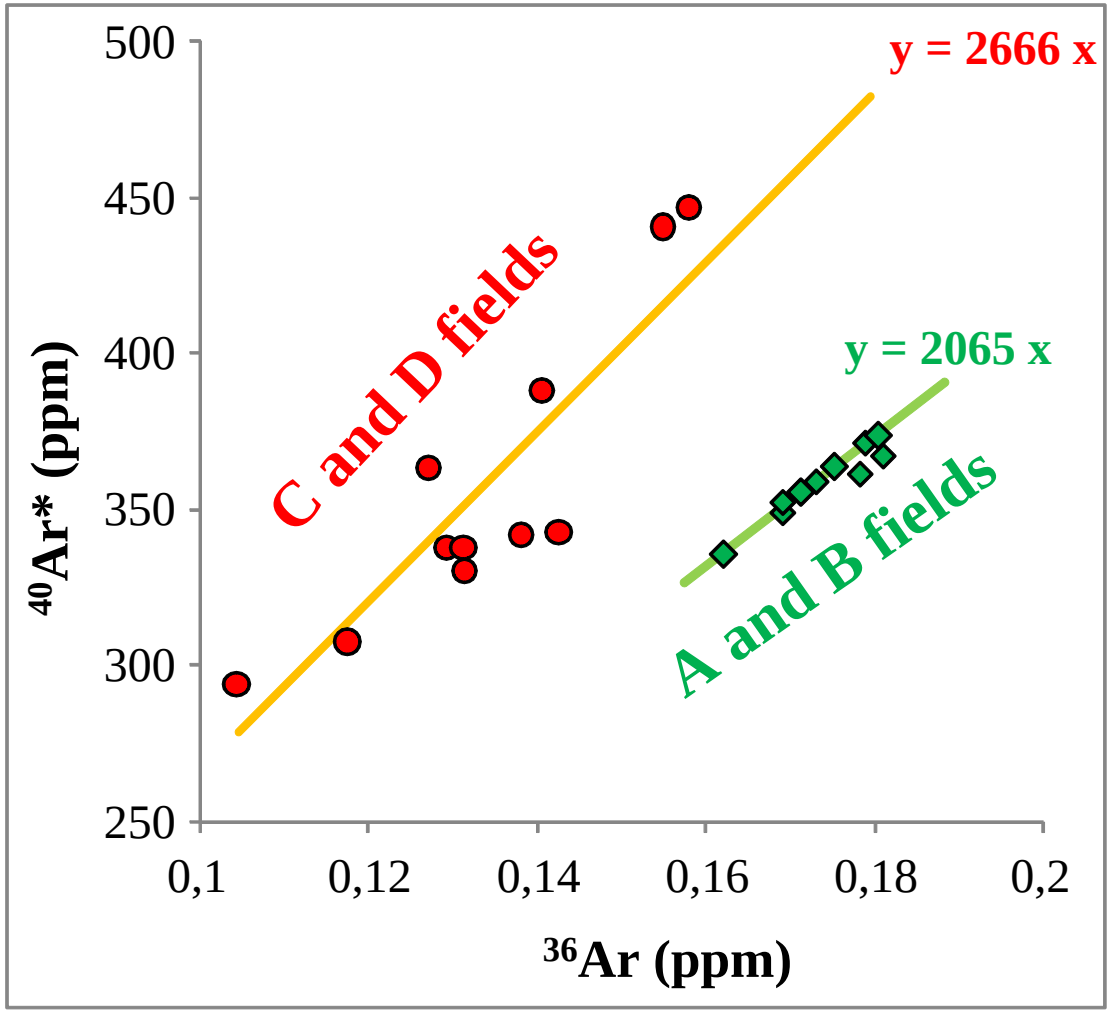
y = 2666 x
y = 2065 x
C and D fields
A and B fields
500
450
400
350
300
250
0,1
0,12
0,14
0,16
0,18
0,2
40Ar* (ppm)
36Ar (ppm)

Figure 15

PRINCIPLE OF THE EFFICIENCY OF ACCUMULATION

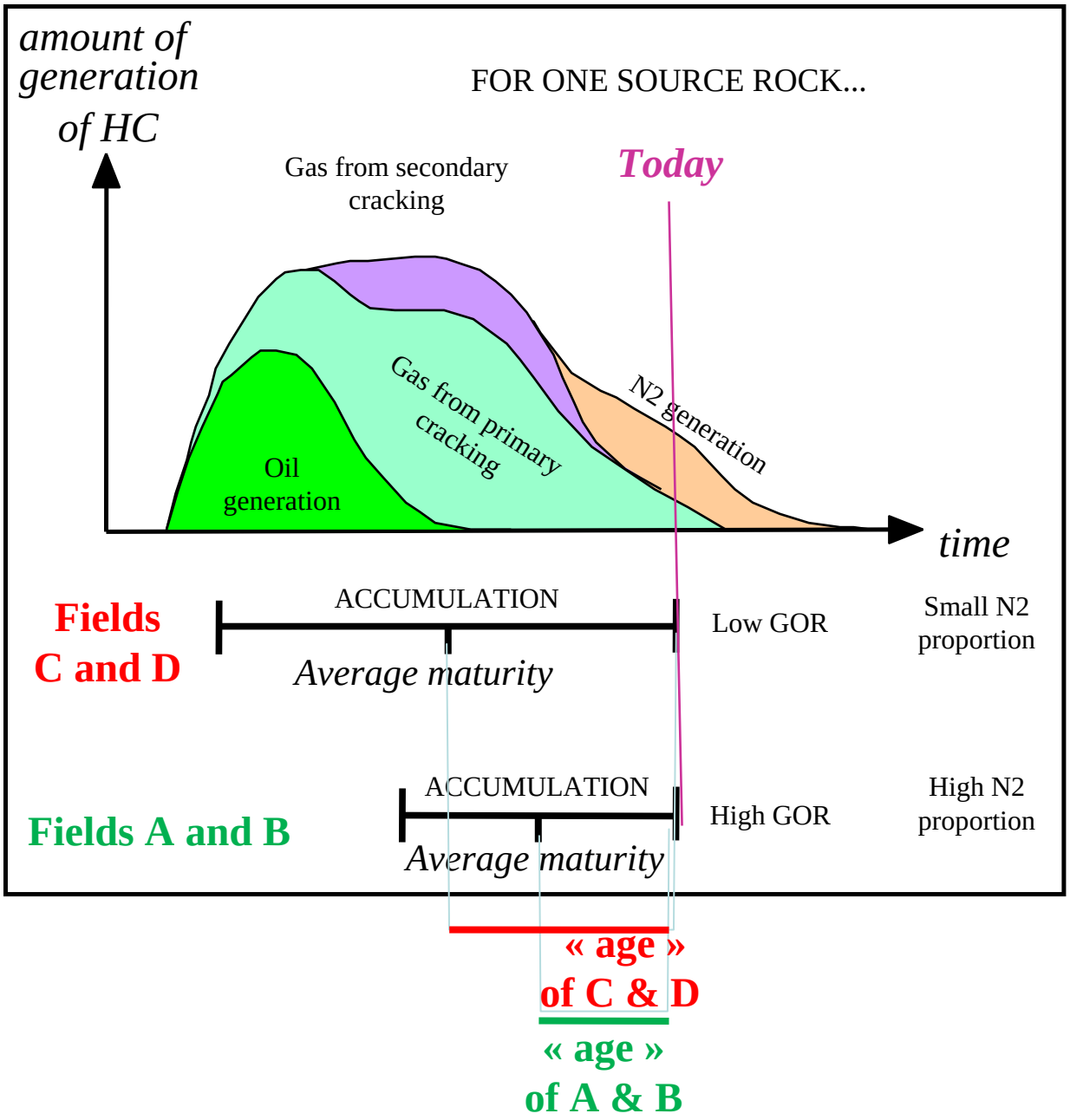

Figure 16

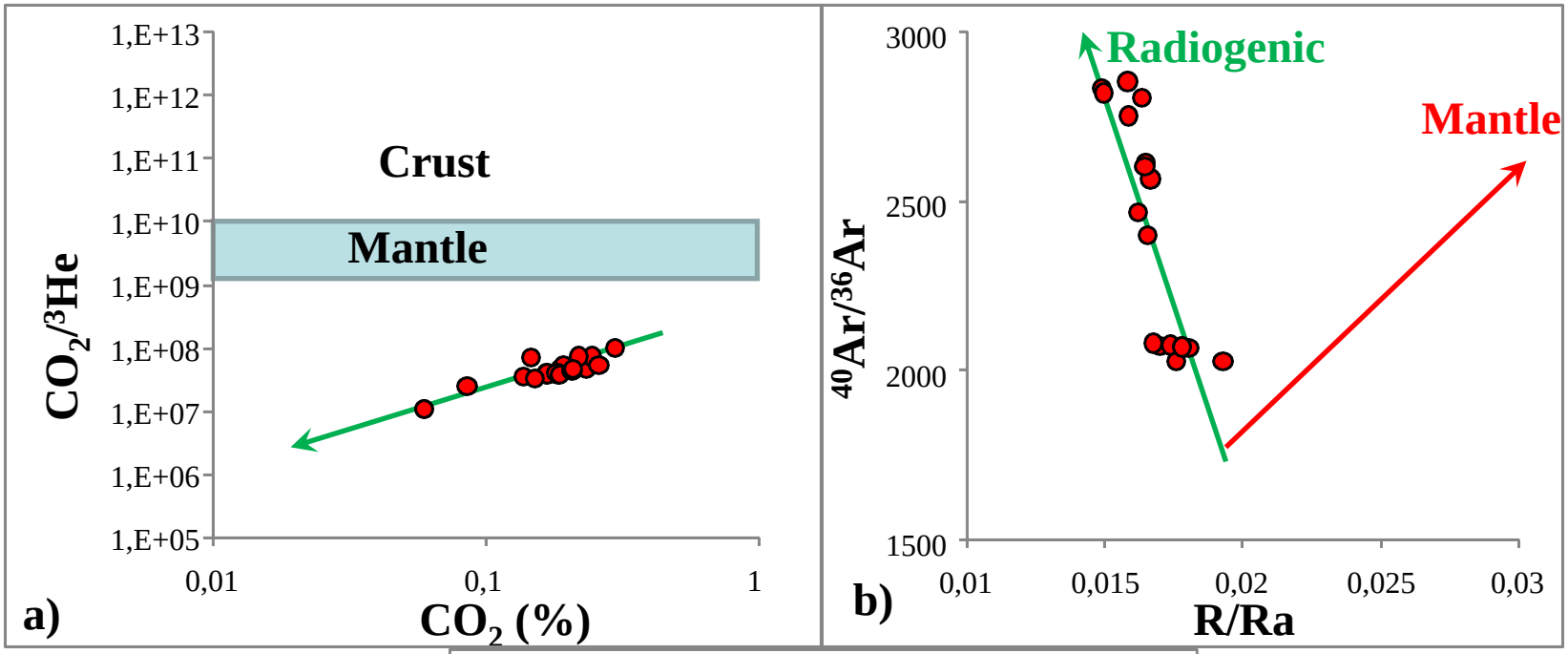

Paleozoic oil and gas accumulations

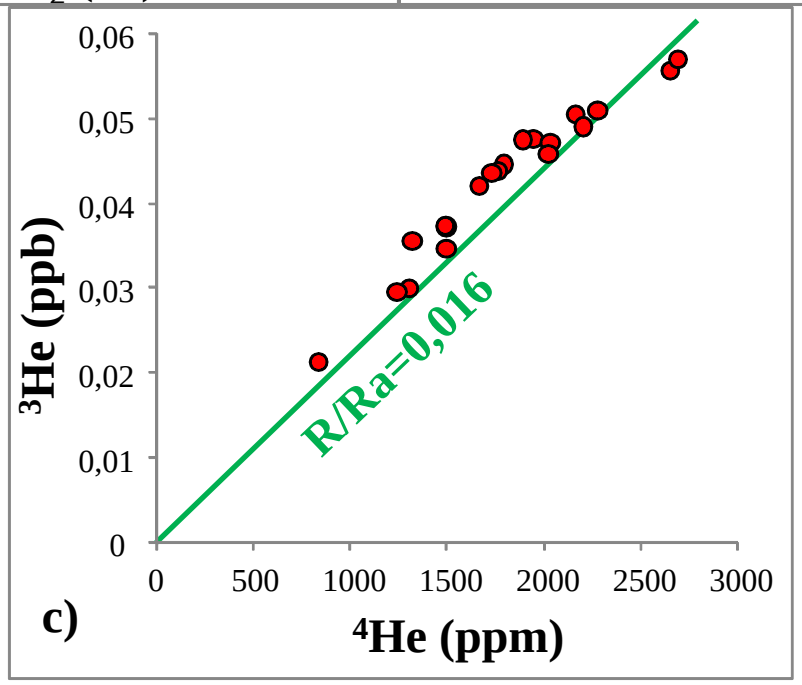

Figure 17

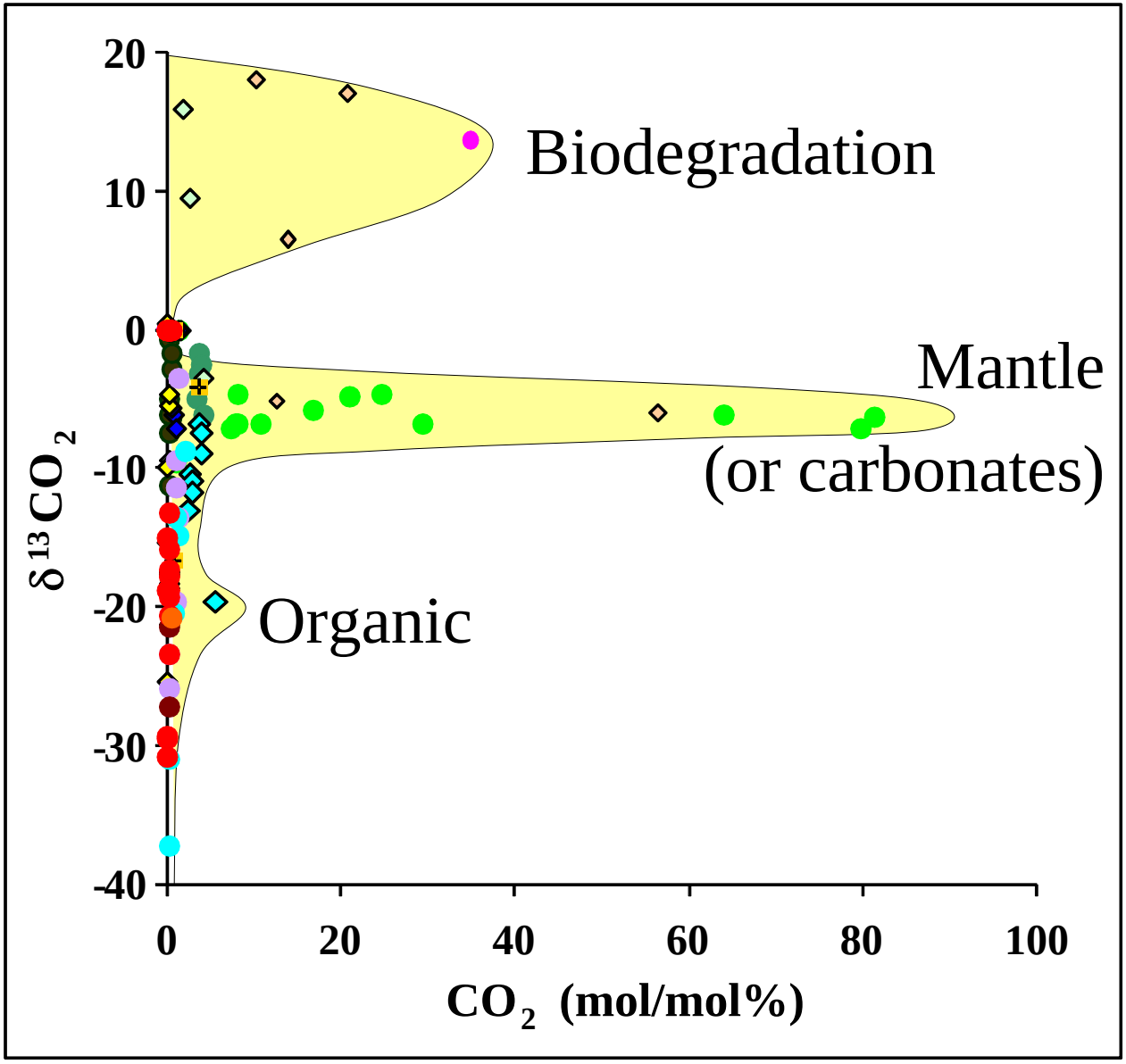
Biodegradation
Mantle
(or carbonates)
Organic
δ13CO2
CO2 (mol/mol%)
20
10
0
-10
-20
-30
-40
0
20
40
60
80
100

Figure 18

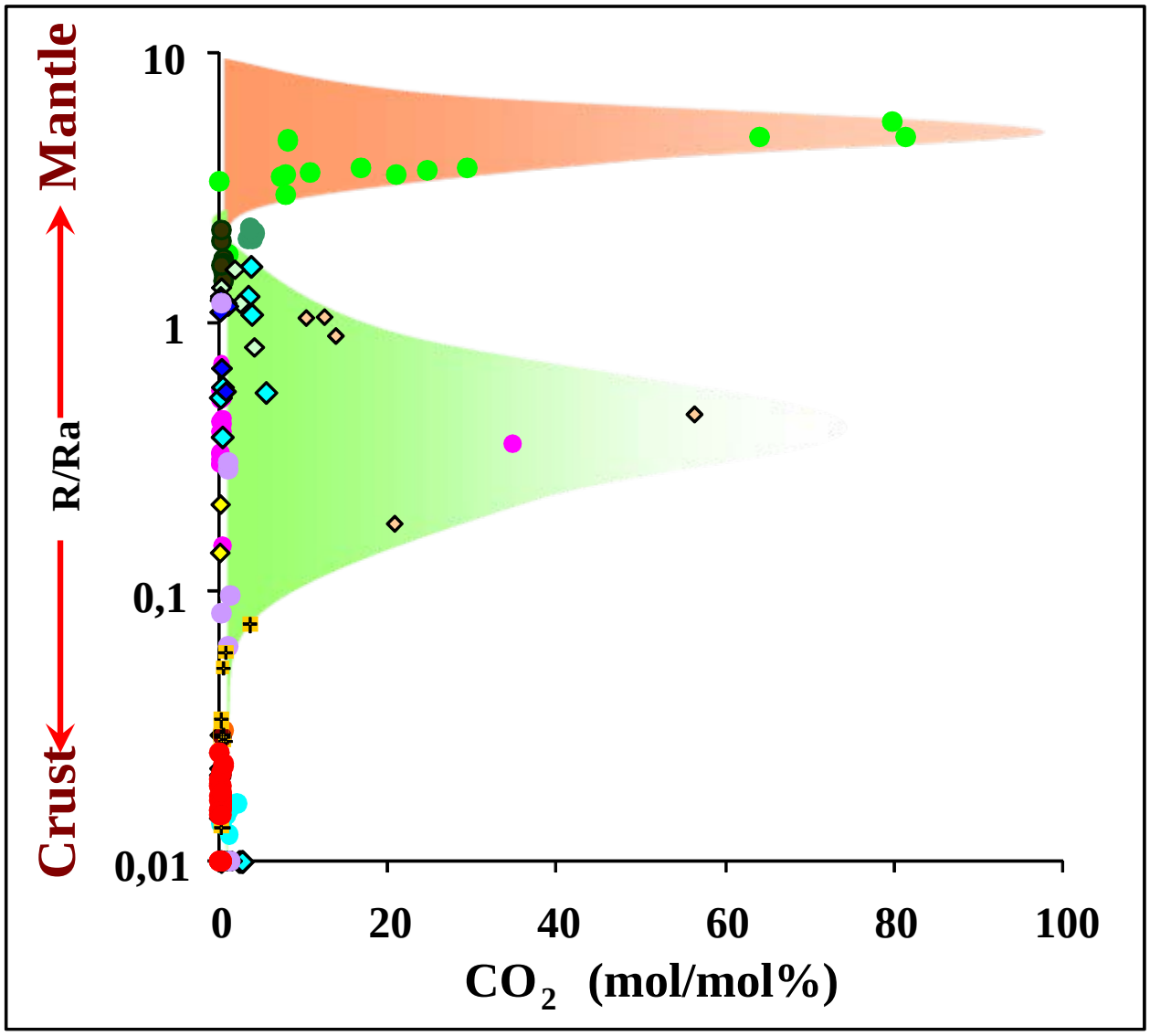

Figure 19

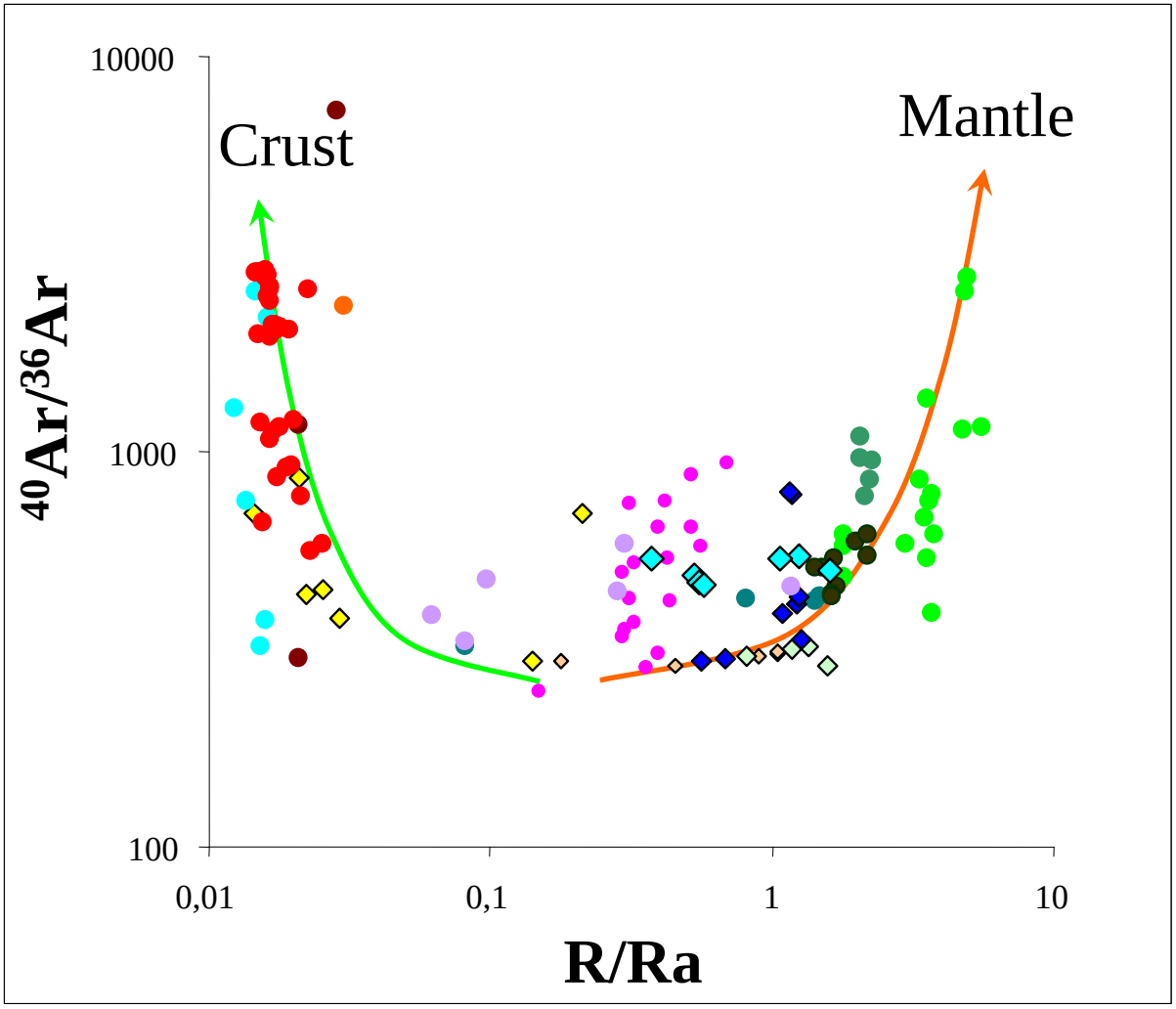

Figure 20

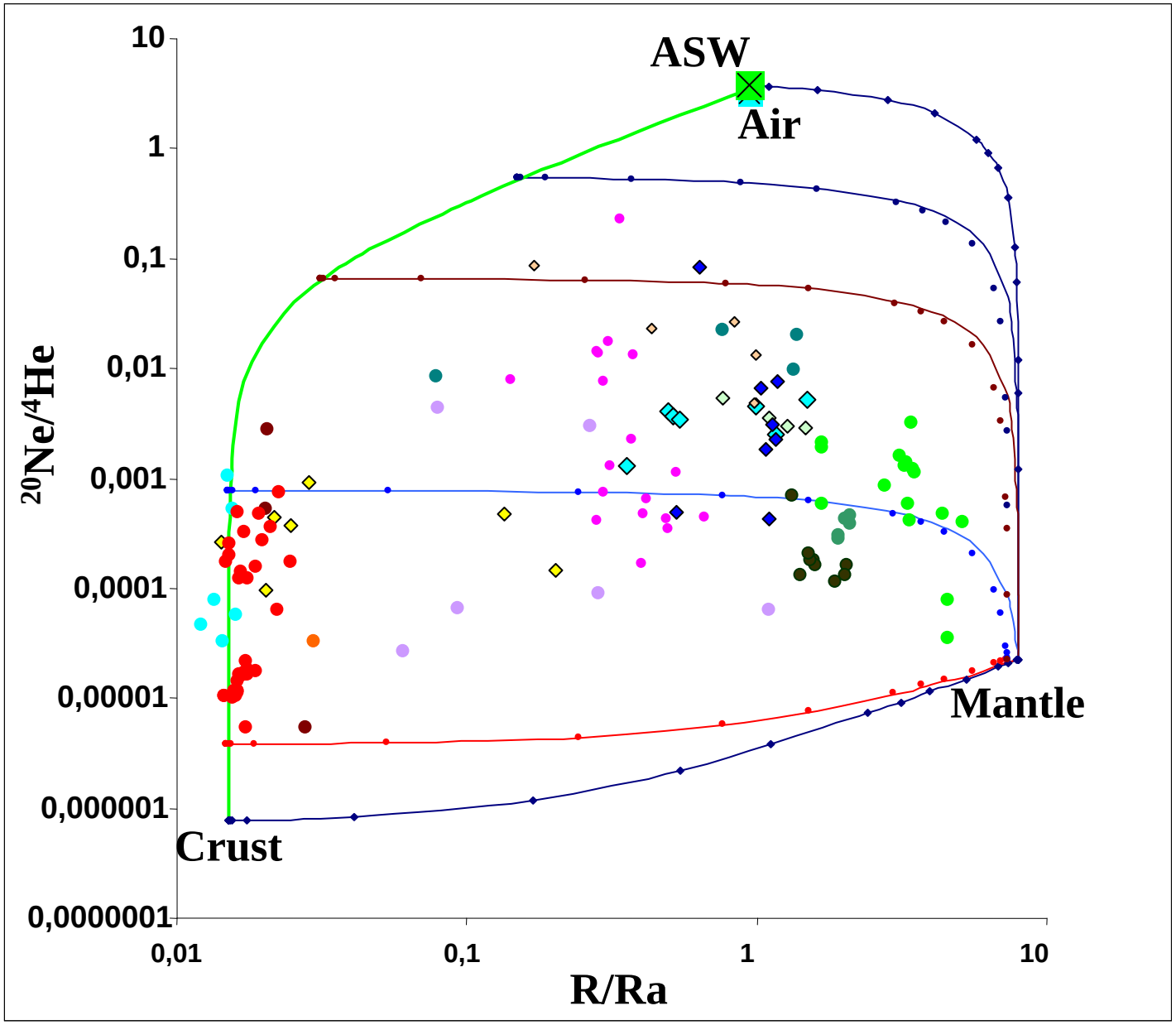
ASW
Air
Mantle
Crust
10
1
0,1
0,01
0,001
0,0001
0,00001
0,000001
0,0000001
$^{20}Ne/^{4}He$
0,01
0,1
1
10
R/Ra

Figure 21

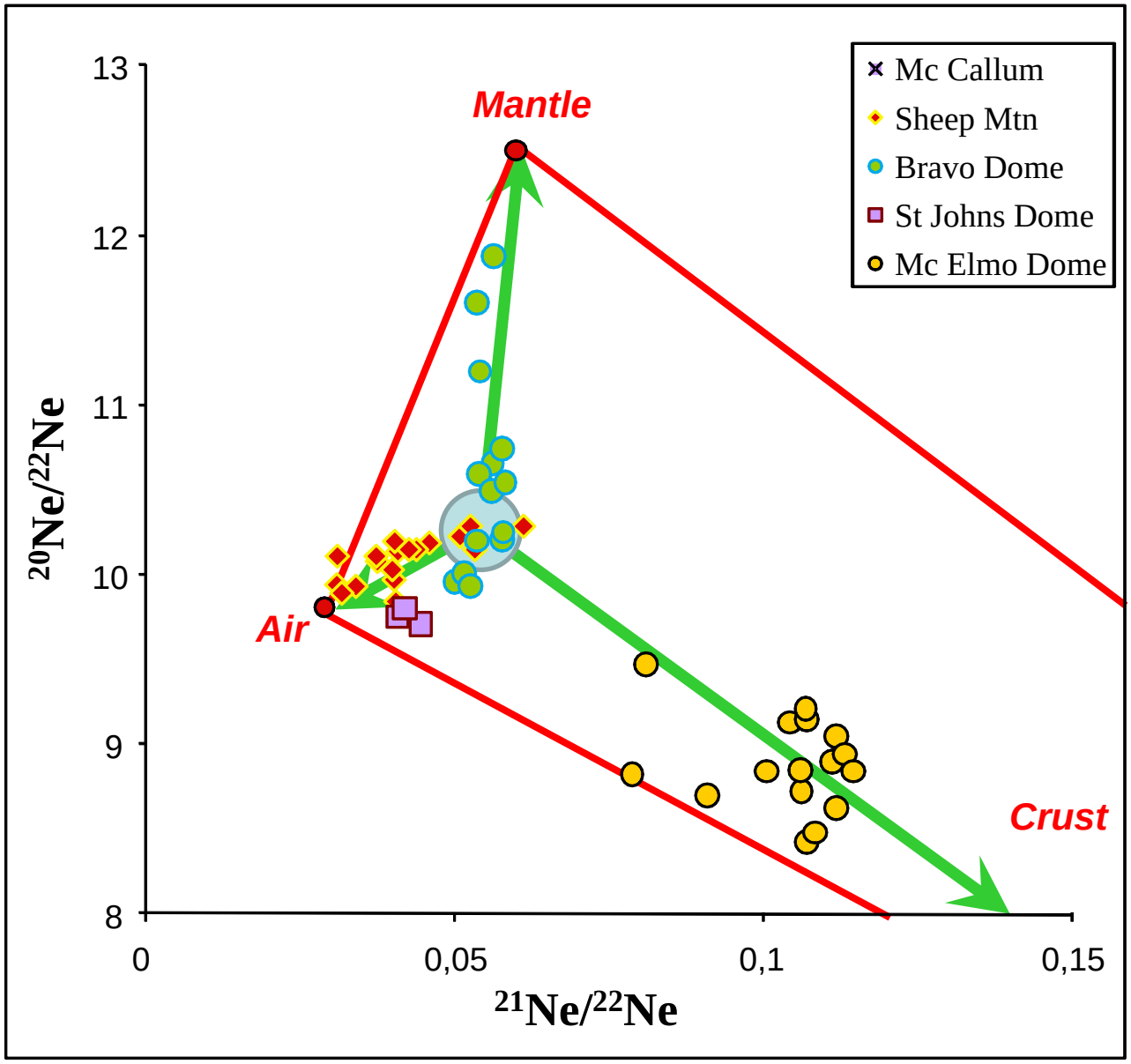
Mc Callum
Sheep Mtn
Bravo Dome
St Johns Dome
Mc Elmo Dome
Mantle
Air
Crust
13
12
11
10
9
8
0
0,05
0,1
0,15
20Ne/22Ne
21Ne/22Ne

Figure 22

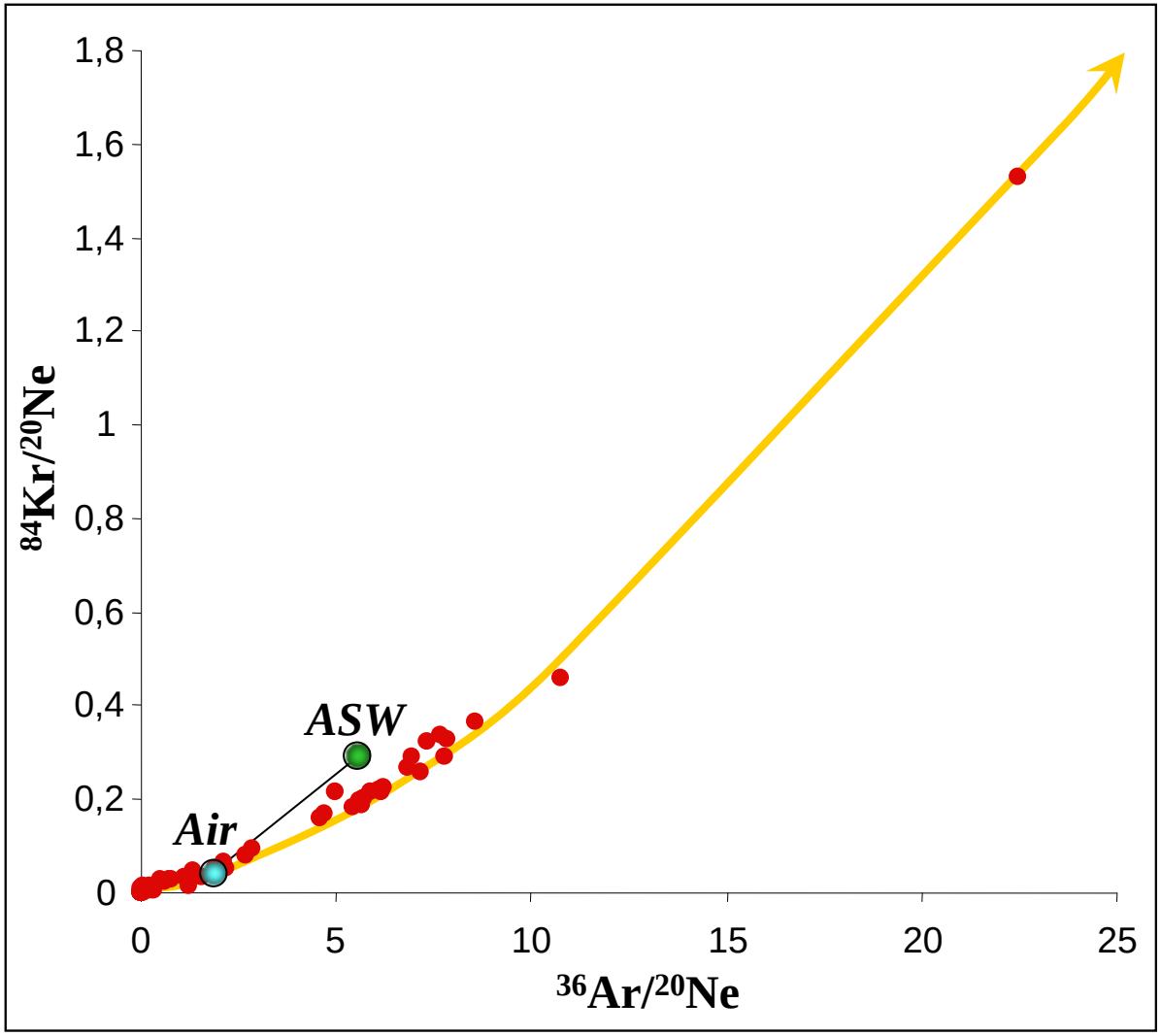
1,8
1,6
1,4
1,2
1
0,8
0,6
0,4
0,2
0
0
5
10
15
20
25
84Kr/20Ne
36Ar/20Ne
ASW
Air

Figure 23

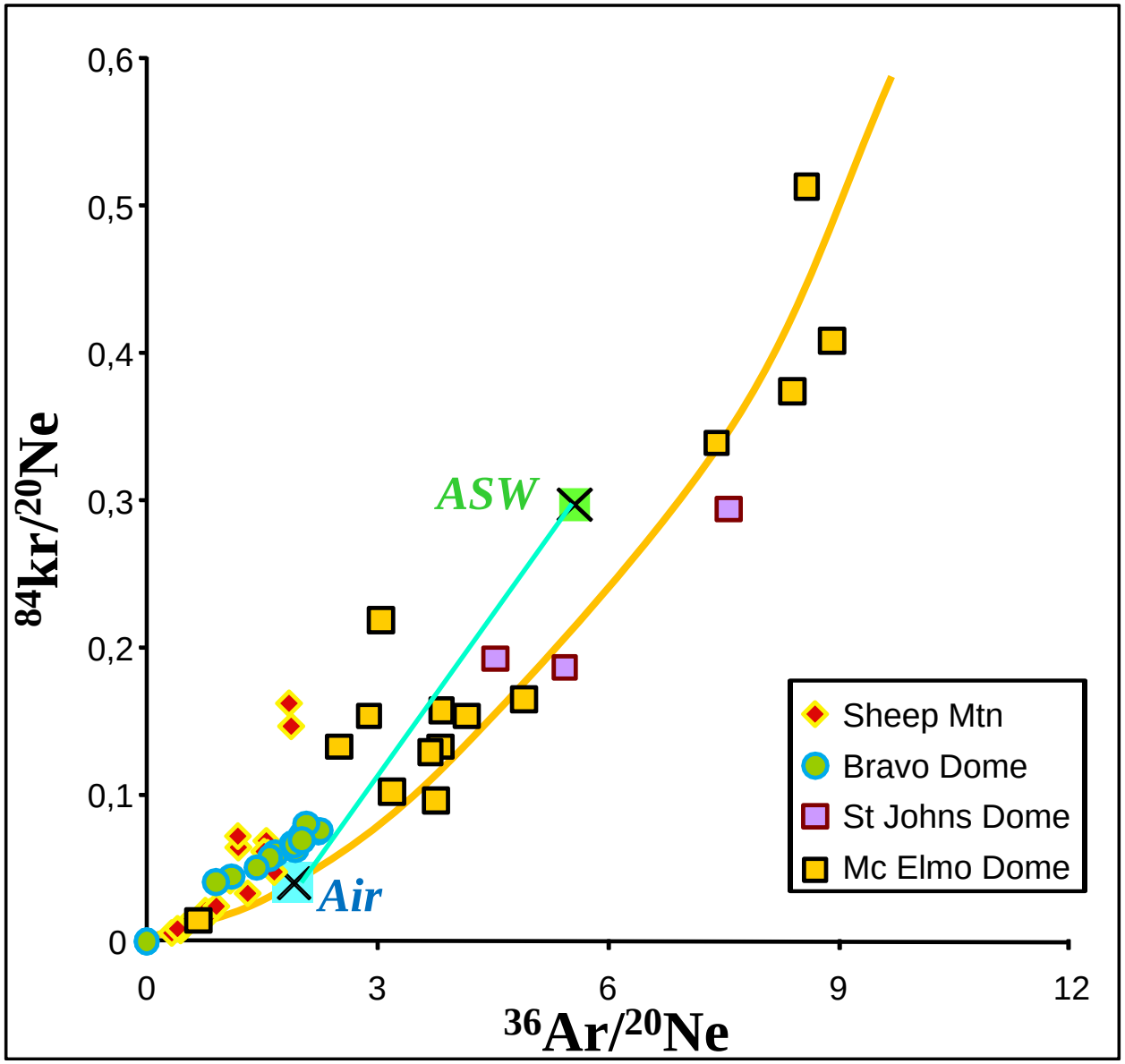
0,6
0,5
0,4
0,3
0,2
0,1
0
0
3
6
9
12
84kr/20Ne
36Ar/20Ne
ASW
Air
Sheep Mtn
Bravo Dome
St Johns Dome
Mc Elmo Dome

Figure 24

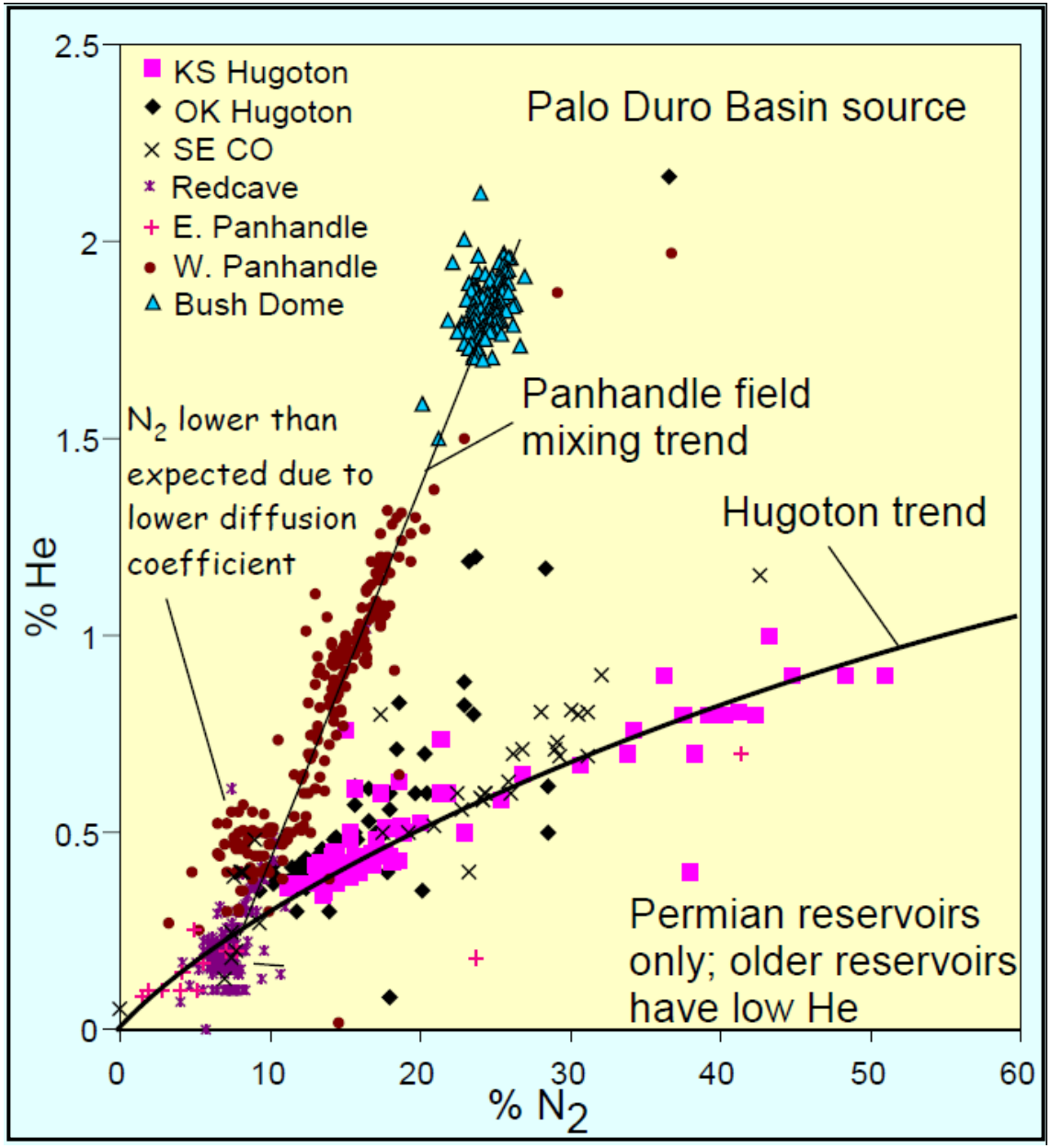
KS Hugoton
OK Hugoton
SE CO
Redcave
E. Panhandle
W. Panhandle
Bush Dome
Palo Duro Basin source
Panhandle field mixing trend
N2 lower than expected due to lower diffusion coefficient
Hugoton trend
Permian reservoirs only; older reservoirs have low He
% He
% N2
0
0.5
1
1.5
2
2.5
0
10
20
30
40
50
60

Figure 25